A SECOND ORDER NUMERICAL CODE FOR PLANE FLOW APPROXIMATION OF OBLIQUE IMPACT

MATHEMATICAL APPLICATIONS GROUP, INCORPORATED

PREPARED FOR
BALLISTIC RESEARCH LABORATORIES

MARCH 1976

BRL CR 294

BRL

AD

CONTRACT REPORT NO. 294

A SECOND ORDER NUMERICAL CODE FOR PLANE FLOW APPROXIMATION OF OBLIQUE IMPACT

Prepared by

Mathematical Applications Group, Inc.
3 Westchester Plaza
Elmsford, NY 10523

March 1976

USA BALLISTIC RESEARCH LABORATORIES
ABERDEEN PROVING GROUND, MARYLAND

UNCLASSIFIED

SECURITY CLASSIFICATION OF THIS PAGE (When Data Entered)

REPORT DOCUMENTATION PAGE		READ INSTRUCTIONS BEFORE COMPLETING FORM
1. REPORT NUMBER BRL CONTRACTOR REPORT NO. 294	2. GOVT ACCESSION NO.	3. RECIPIENT'S CATALOG NUMBER
4. TITLE (and Subtitle) A Second Order Numerical Code for Plane Flow Approximation of Oblique Impact		5. TYPE OF REPORT & PERIOD COVERED Final 6. PERFORMING ORG. REPORT NUMBER P-7110
7. AUTHOR(s) S. Z. Burstein H. S. Schechter		8. CONTRACT OR GRANT NUMBER(s) DAAD05-75-C-0740
9. PERFORMING ORGANIZATION NAME AND ADDRESS Mathematical Applications Group, Inc. 3 Westchester Plaza Elmsford, NY 10523		10. PROGRAM ELEMENT, PROJECT, TASK AREA & WORK UNIT NUMBERS
11. CONTROLLING OFFICE NAME AND ADDRESS US Army Ballistic Research Laboratories Aberdeen Proving Ground, MD 21005		12. REPORT DATE MARCH 1976 13. NUMBER OF PAGES 49
14. MONITORING AGENCY NAME & ADDRESS (if different from Controlling Office) US Army Materiel Development and Readiness Command 5001 Eisenhower Avenue Alexandria, VA 22333		15. SECURITY CLASS. (of this report) UNCLASSIFIED 15a. DECLASSIFICATION/DOWNGRADING SCHEDULE

16. DISTRIBUTION STATEMENT (of this Report)

Approved for public release; distribution unlimited.

17. DISTRIBUTION STATEMENT (of the abstract entered in Block 20, if different from Report)

18. SUPPLEMENTARY NOTES

19. KEY WORDS (Continue on reverse side if necessary and identify by block number)

penetration
perforation
oblique impact
plane flow

20. ABSTRACT (Continue on reverse side if necessary and identify by block number)

This report describes modifications completed for the SMITE code in transforming the axisymmetric version to plane flow. Details of several test calculations are also presented.

DD FORM 1 JAN 73 1473 EDITION OF 1 NOV 65 IS OBSOLETE

UNCLASSIFIED

SECURITY CLASSIFICATION OF THIS PAGE (When Data Entered)

Destroy this report when it is no longer needed.
Do not return it to the originator.

Secondary distribution of this report by originating or sponsoring activity is prohibited.

Additional copies of this report may be obtained from the National Technical Information Service, U.S. Department of Commerce, Springfield, Virginia 22151.

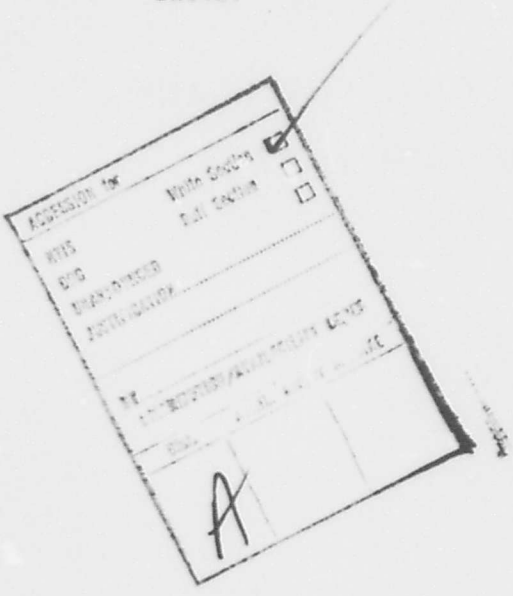

The findings in this report are not to be construed as an official Department of the Army position, unless so designated by other authorized documents.

TABLE OF CONTENTS

I. INTRODUCTION

This report describes the modifications completed for the SMITE Code in transforming the axisymmetric version to plane flow. The reader should refer to BRL Contract Report No. 239 for a more detailed description of the method of analysis. Several test calculations have been carried out at 65° angle of attack and are reported upon.

II.

Basic Differential Equations

a) Plane Strain Elastic Model

When a material supports shear stresses, it is necessary to include, in addition to the pressure forces, terms which account for the presence of these stresses. The equations of motion for such a material can be derived by applying the physical laws describing the conservation of mass, momentum and energy to a finite element of the material body. In addition, a statement of the stress-strain relationship of the material is required. For this paper a linear theory is assumed, i.e. material bodies will satisfy Hooke's law. Then these laws may be usefully written as a set of partial differential equations in a cartesian coordinate system, as follows. If the substantial or particle derivative is defined as

$$\frac{d}{dt} = \frac{\partial}{\partial t} + u \frac{\partial}{\partial x} + v \frac{\partial}{\partial y}$$

then the conservation of mass can be written in terms of the density (the mass per unit volume) ρ, and the divergence of the velocity field, with components u and v in the x and y direction respectively as

$$\frac{d\rho}{dt} = - \rho \left(\frac{\partial u}{\partial x} + \frac{\partial v}{\partial y} \right) \qquad (2.1)$$

The two momentum laws reflect the appearance of the stress components τ_{ij}. The x-component of the momentum satisfies

$$\rho \frac{du}{dt} = \frac{\partial \tau_{11}}{\partial x} + \frac{\partial \tau_{12}}{\partial y} \qquad (2.2)$$

and the y-component of the momentum satisfies

$$\rho \frac{dv}{dt} = \frac{\partial \tau_{12}}{\partial x} + \frac{\partial \tau_{22}}{\partial y} \qquad (2.3)$$

The evolution equation for the internal energy, e, per unit volume is given by

$$\rho \frac{de}{dt} = \tau_{11} \frac{\partial u}{\partial x} + \tau_{22} \frac{\partial v}{\partial y} + \tau_{12} \left(\frac{\partial v}{\partial x} + \frac{\partial u}{\partial y} \right) \qquad (2.4)$$

The stresses required in the above relations must be obtained from the strains and strain rates. The linear stress-strain laws, with correction for rotation, are usually written in terms of deviator stresses S_{ij}. The rate of change of the stress component S_{ij} are given in terms of the strain rate, $\dot{e}_{ij}$, via

$$\frac{dS_{11}}{dt} = \frac{2\mu}{3}\left(2\frac{\partial u}{\partial x} - \frac{\partial v}{\partial y}\right) + \tau_{12}\left(\frac{\partial u}{\partial y} - \frac{\partial v}{\partial x}\right) \tag{2.5}$$

$$\frac{dS_{12}}{dt} = \mu\left(\frac{\partial u}{\partial y} + \frac{\partial v}{\partial x}\right) - \frac{S_{11}-S_{22}}{2}\left(\frac{\partial u}{\partial y} - \frac{\partial v}{\partial x}\right) \tag{2.6}$$

$$\frac{dS_{22}}{dt} = \frac{2\mu}{3}\left(2\frac{\partial v}{\partial y} - \frac{\partial u}{\partial x}\right) - \tau_{12}\left(\frac{\partial u}{\partial y} - \frac{\partial v}{\partial x}\right) \tag{2.7}$$

$$\frac{dS_{33}}{dt} = -\frac{2\mu}{3}\left(\frac{\partial u}{\partial x} + \frac{\partial v}{\partial y}\right) \tag{2.8}$$

The above Hookian laws, Equations (2.5) - (2.8), are connected to the evolution laws (2.1) - (2.4) by the algebraic conditions

$$\tau_{ij} = S_{ij} - p\delta_{ij} \qquad \delta_{ij} = 1 \text{ for } i = j$$

$$= 0 \text{ otherwise} \tag{2.9 - 2.11}$$

The pressure p is related to the density ρ and specific internal energy e through the equation of state

$$p = P(\rho, e) \tag{2.12}$$

The above set form a system of twelve equations for the twelve unknowns ρ, u,v,e,p, τ_{11}, τ_{12}, τ_{22}, τ_{33}, S_{11}, S_{22} and S_{33}.

At this point we show that Equations (2.1) - (2.12) form a system which is not self consistent. To see this add Equations (2.5), (2.7) and (2.8). It is clear then that the sum

$\sum_{i=1}^{3} S_{ii}$ satisfies

$$\frac{d}{dt}\left(S_{11} + S_{22} + S_{33}\right) = 0 \tag{2.13}$$

which implies that the sum of these stress deviators is a constant of the motion of the material; without loss of generality this constant can be taken to be zero for at t=0 each $S_{ii}=0$. Thus

$$\sum_{i=1}^{3} S_{ii} = 0 \tag{2.14}$$

for all time.

Now if we sum Equations (2.9) through (2.11) for i=j, we obtain the relation

$$\tau_{11} + \tau_{22} + \tau_{33} = S_{11} + S_{22} + S_{33} - 3p \tag{2.15}$$

which yields, after satisfying Equation (2.14),

$$\tau_{11} + \tau_{22} + \tau_{33} = - 3p \tag{2.16}$$

Equation (2.16) states that the pressure p is determined by the mean of the stress tensor. This is a contradiction of Equation (2.12) which states the pressure is a function only of the density and internal energy.

Hooke's laws can be written in the form

$$\tau_{ii} = 2\mu e_{ii} + \lambda \sum_{j} e_{jj} \qquad i = 1,2,3 \tag{2.17}$$

$$\tau_{ij} = 2\mu e_{ij}$$

Here μ is the shear modulus of the material, λ is a Lamé constant and the strain e_{ij} is defined by

$$e_{ij} = \frac{1}{2} \left(\frac{\partial \bar{x}_i}{\partial x_j} + \frac{\partial \bar{x}_j}{\partial x_i} \right) \tag{2.18}$$

The displacements are $\bar{x}_i$.

Differentiating Equations (2.17) and (2.18) with respect to time yields

$$\dot{\tau}_{ii} = 2\mu \dot{e}_{ii} + \lambda \sum_{j} \dot{e}_{jj} \tag{2.19}$$

$$\dot{\tau}_{ij} = 2\mu \dot{e}_{ij}$$

The corresponding strain rate tensor is then given in terms of the velocity gradient,

$$\dot{e}_{ij} = \frac{1}{2} \left(\frac{\partial u_i}{\partial x_j} + \frac{\partial u_j}{\partial x_i} \right)$$

with u_i and u_j the components of the velocity.

If Equation (2.16) is differentiated with respect to time we can compute $\dot{p}$; using Equation (2.19) for $\dot{\tau}_{ii}$ we obtain:

$$\dot{p} = -\frac{1}{3} \Sigma \dot{\tau}_{ii}$$

$$= -\frac{1}{3} \left(2\mu \Sigma \dot{e}_{ii} + 3\lambda \Sigma \dot{e}_{ii} \right)$$

$$= -\frac{2\mu+3\lambda}{3} \Sigma \dot{e}_{ii} = -k \operatorname{div} \bar{u}$$

which, in cartesian coordinates, yields for the rate of change of the pressure

$$\dot{p} = -k \left(\frac{\partial u}{\partial x} + \frac{\partial v}{\partial y} \right) \qquad (2.20)$$

We have defined the constant k, the bulk modulus, in terms of the Lamé constants μ and λ.

Clearly Equation (2.20), obtained from Hooke's law is not consistent with Equation (2.12). In fact Equation (2.20) together with Equation (2.1) yields

$$\frac{dp}{dt} = \frac{k}{\rho} \frac{d\rho}{dt}$$

which can be integrated from the lower limit $(p, \rho)=(0,\rho_0)$ to the state (p, ρ); this yields for the pressure

$$p = k \operatorname{Ln}(1+\mu) \quad , \quad \mu = \frac{\rho}{\rho_0} - 1 \qquad (2.21)$$

Equation (2.21) can be expanded in a Taylor series for $\rho/\rho_0 \sim 1$ to obtain a polynomial for p as a function of μ.

Thus, Equation (2.12) should, for consistency, be close to Equation (2.21) but obviously cannot in general be the same. To be consistent then, there is really no degree of freedom in the choice of the form for an equation of state, Equation (2.12), in the system (2.1) - (2.12).

One possible way to avoid the above inconsistency is to replace the stresses τ_{ij} appearing in Equations (2.1) - (2.4) by the deviatoric stresses S_{ij} and the pressure p through the use of Equations (2.9) - (2.11) and then eliminate Equations (2.9) - (2.11). The stress deviator S_{33} can also be eliminated by using Equation (2.14). The resulting set of equations can be written as

$$\frac{d\rho}{dt} = - \rho\left(\frac{\partial u}{\partial x} + \frac{\partial v}{\partial y}\right) \tag{2.22}$$

$$\rho \frac{du}{dt} = - \frac{\partial p}{\partial x} + \frac{\partial S_{11}}{\partial x} + \frac{\partial S_{12}}{\partial y} \tag{2.23}$$

$$\rho \frac{dv}{dt} = - \frac{\partial p}{\partial y} + \frac{\partial S_{12}}{\partial x} + \frac{\partial S_{22}}{\partial y} \tag{2.24}$$

$$\rho \frac{de}{dt} = (S_{11}-p) \frac{\partial u}{\partial x} + (S_{22}-p) \frac{\partial v}{\partial y} + S_{12} \left(\frac{\partial v}{\partial x} + \frac{\partial u}{\partial y}\right) \tag{2.25}$$

$$\frac{dS_{11}}{dt} = \frac{2\mu}{3} \left(2\frac{\partial u}{\partial x} - \frac{\partial v}{\partial y}\right) + S_{12} \left(\frac{\partial u}{\partial y} - \frac{\partial v}{\partial x}\right) \tag{2.26}$$

$$\frac{dS_{12}}{dt} = \mu\left(\frac{\partial u}{\partial y} + \frac{\partial v}{\partial x}\right) - \frac{S_{11}-S_{22}}{2} \left(\frac{\partial u}{\partial y} - \frac{\partial v}{\partial x}\right) \tag{2.27}$$

$$\frac{dS_{22}}{dt} = \frac{2\mu}{3} \left(2\frac{\partial v}{\partial y} - \frac{\partial u}{\partial x}\right) - S_{12} \left(\frac{\partial u}{\partial y} - \frac{\partial v}{\partial x}\right) \tag{2.28}$$

$$p = P(\rho, e) \tag{2.29}$$

Thus we have eight equations for the eight unknowns ρ, u, v, e, S_{11}, S_{12}, S_{22}, and p. Equations (2.22) - (2.29) are consistent. The only disadvantage of this set of equations is that Hooke's law of linear elasticity can not be recovered. This is due to the fact that the pressure in Equation (2.29) is the thermodynamic pressure while Hooke's law does not attempt to include thermodynamic effects. If nonadiabatic terms are included so as to produce a modified Hooke's law then the relation (2.21) would be modified to include temperature effects while the stress deviators S_{ij} would be unchanged. Hence the quantities S_{ij} in Equations (2.22) - (2.29) are the stress deviators and an additional constant, i.e. k in Equation (2.20) (in addition to the shear modulus μ), usually encountered in two dimensional linear elasticity, is eliminated by the inclusion of an equation of state (2.29)

b) A Plastic Model

Equations (2.26) - (2.28) express the stress-strain relations for a material behaving with linear elastic properties. Before we proceed, we first rewrite these equations in a more convenient form. We define the derivative $\frac{D}{Dt}$ to be a tensor operator unaffected by rotations. Then, we construct this operator from the substantial derivative of the stress deviators

$$\frac{DS_{11}}{Dt} = \frac{dS_{11}}{dt} - S_{12}\left(\frac{\partial u}{\partial y} - \frac{\partial v}{\partial x}\right)$$

$$\frac{DS_{12}}{Dt} = \frac{dS_{12}}{dt} + \frac{S_{11}-S_{22}}{2}\left(\frac{\partial u}{\partial y} - \frac{\partial v}{\partial x}\right) \qquad (2.30)$$

$$\frac{DS_{22}}{Dt} = \frac{dS_{22}}{dt} + S_{12}\left(\frac{\partial u}{\partial y} - \frac{\partial v}{\partial x}\right)$$

The time derivatives of the strain deviators can be written using the definitions:

$$\dot{\varepsilon}_{11} = \frac{\partial u}{\partial x} - \frac{1}{3}\left(\frac{\partial u}{\partial x} + \frac{\partial v}{\partial y}\right)$$

$$= \frac{2}{3}\frac{\partial u}{\partial x} - \frac{1}{3}\frac{\partial v}{\partial y} \qquad (2.31)$$

$$\dot{\varepsilon}_{22} = \frac{\partial v}{\partial y} - \frac{1}{3}\left(\frac{\partial u}{\partial x} + \frac{\partial v}{\partial y}\right)$$

$$= -\frac{1}{3}\frac{\partial u}{\partial x} + \frac{2}{3}\frac{\partial v}{\partial y}$$

$$\dot{\varepsilon}_{12} = \frac{1}{2}\left(\frac{\partial u}{\partial y} + \frac{\partial v}{\partial x}\right)$$

Then, Equations (2.26) - (2.28) can be written so that the deviator stress components of the stress tensor are obtained from the deviator strain components of the strain tensor, i.e.,

$$\frac{DS_{11}}{Dt} = 2\mu\dot{\varepsilon}_{11}$$

$$\frac{DS_{12}}{Dt} = 2\mu\dot{\varepsilon}_{12} \qquad (2.32)$$

$$\frac{DS_{22}}{Dt} = 2\mu\dot{\varepsilon}_{22}$$

Equations (2.32 are applicable only in the elastic region of flow. In general a material which exhibits a linear variation of strain with stress is called linear elastic. However at the proportional limit the strain may increase more rapidly with increasing stress. In this region, the material deforms plastically. If the strain is allowed to increase with no increase in the stress the material is called perfectly plastic. If some variation in stress occurs the material is experiencing work hardening.

A material when exposed to external loading can experience permanent deformation as stresses exceed certain characteristic limits of the material. A tacit assumption is made in elastic theory: the assumption that a scalar function $f(\tau_{ij}, \varepsilon^p_{ij}, \omega)$ called a yield function, exists. Arguments τ_{ij}, ε^p_{ij} and ω correspond to the stress state, the plastic strain and a measure of the loading history respectively.

The equation

$$f = 0$$

represents a surface in stress space; for $f < 0$ the change in plastic deformation is zero while only when $f=0$ is plastic deformation allowed to occur. If the material properties are independent of strain rate, $f > 0$ has no meaning. In the plastic region, in place of System (2.32), we invoke the Prandtl-Reuss formulation for plastic flow.

In a mixed elastic plastic flow material System (2.32) applies whenever

$$\Sigma \quad S_{ij}^2 = 2\,(S_{11}^2 + S_{22}^2 + S_{11}S_{22} + S_{12}^2) < 2K^2 \qquad (2.33)$$

$1 \leq i, \quad j \leq 3$

with K^2 a constant of the material. However, whenever the von Mises yield condition, based on the assumed form for the yield function $f=f(\Sigma S_{ij})$, requires that

$$\Sigma S_{ij}^2 \geq 2K^2 \qquad (2.34)$$

be satisfied, then System (2.32) is replaced by a viscoelastic model system patented after a viscoelastic constitutive relation of the form

$$\frac{DS_{11}}{Dt} = 2\mu(\dot{\epsilon}_{11} - \lambda S_{11})$$

$$\frac{DS_{12}}{Dt} = 2\mu(\dot{\epsilon}_{12} - \lambda S_{12}) \qquad (2.35)$$

$$\frac{DS_{22}}{Dt} = 2\mu(\dot{\epsilon}_{22} - \lambda S_{22})$$

Now the constant λ is determined by requiring equality in the von Mises yield criterion (2.34) rather than setting it to $1/2\,\rho\nu$, ν the kinematic viscosity of the material. Multiply each Equation (2.35) by S_{ij} and sum:

$$\frac{1}{2}\,\Sigma\,\frac{DS_{ij}^2}{Dt} = 2\mu \quad (\Sigma S_{ij}\dot{\epsilon}_{ij} - \lambda \Sigma S_{ij}^2) \qquad (2.36)$$

Now use the fact that $\Sigma S_{ij}^2 = 2K^2 = \text{constant}$. Equation (2.36) can then be solved explicitly for λ,

$$\lambda = \frac{1}{2K^2} \Sigma S_{ij} \dot{\epsilon}_{ij} \tag{2.37}$$

In cartesian coordinates (2.37) can be expressed as

$$\lambda = \frac{1}{2K^2} \left\{ S_{11} \left[u_x - 1/3 \, (u_{xx} + v_{yy}) \right] + S_{22} \left[v_y - 1/3 \, (u_{xx} + v_{yy}) \right] + S_{12} \, (u_y + v_x) + (S_{11} + S_{22}) \left[1/3 \, (u_{xx} + v_{yy}) \right] \right\}$$

$$= \frac{1}{2K^2} \left\{ S_{11} \, u_{xx} + S_{22} v_{yy} + S_{12} \left(\frac{u_y + v_x}{2} \right) \right\} \tag{2.37'}$$

Here we have used the notation $\frac{\partial u}{\partial x} = u_x$, etc.

In this way both the elastic and plastic regions can be described by Equation (2.35). The prescriptior is

$$\text{Elastic} \begin{cases} \Sigma S_{ij}^2 < 2K^2 \quad \text{or} \quad \Sigma S_{ij}^2 = 2K^2 \\ \lambda = 0 \qquad\qquad \Sigma S_{ij} \dot{\epsilon}_{ij} \leq 0 \text{ (unloading)} \end{cases} \tag{2.38}$$

$$\text{Plastic} \begin{cases} \Sigma S_{ij}^2 = 2K^2 \\ \lambda = \frac{1}{2K^2} \Sigma S_{ij} \dot{\epsilon}_{ij} > 0 \end{cases} \tag{2.39}$$

Equations (2.38) and (2.39) show that, in the plastic region, if one begins on the material yield surface, and in the absence of unloading, then one remains on the yield surface.

Because of the complicated boundary conditions together with the nonlinearities of Equations (2.38) and (2.39) this system must be solved numerically. If one uses a finite difference technique in the plastic region then the truncation errors inherent in any difference scheme will result in a set of deviatoric stresses which no longer lie on the yield surface. It is therefore necessary to change the finite difference schemes in the plastic region to insure that unloading does not occur due to truncation errors. Thus, λ in the numerical method will not strictly be determined by Equation (2.39) but instead the derivation of this formula will be used to force the yield condition to be satisfied numerically.

In order to describe the method used, which is second order accurate, we assume that a solution is known at time t and we wish to determine the solution at time $t + \Delta t$. The solution to Equation (2.40) with $\lambda = 0$ (i.e. the elastic case) will be denoted by S^e_{ij}. Then, by using a backward Taylor series in time one has

$$S_{ij}(t) = S_{ij}(t+\Delta t) - \Delta t\, \dot{S}_{ij}(t+\Delta t) + \frac{(\Delta t)^2}{2}\, \ddot{S}_{ij}(t+\Delta t) + \mathcal{O}((\Delta t)^3)$$

or

$$S_{ij}(t+\Delta t) = S_{ij}(t) + \Delta t\, \dot{S}_{ij}(t+\Delta t) - \frac{(\Delta t)^2}{2}\, \ddot{S}_{ij}(t+\Delta t) + \mathcal{O}((\Delta t)^3) \qquad (2.40)$$

Using the differential Equation (2.35) in Equation (2.40) yields

$$S_{ij}(t+\Delta t) = S_{ij}(t) + 2\Delta t\mu \left[\dot{\varepsilon}_{ij}(t+\Delta t) - \lambda(t+\Delta t) S_{ij}(t+\Delta t)\right] - 2\mu \frac{(\Delta t)^2}{2} \left[\dot{\varepsilon}_{ij}(t+\Delta t) - \frac{\lambda(t+\Delta t) S_{ij}(t+\Delta t) - \lambda(t) S_{ij}(t)}{\Delta t}\right] \qquad (2.41)$$

Or introducing the elastic deviatoric stresses, S^e_{ij}, Equation (2.41) can be written as

$$S_{ij}(t+\Delta t) = S^{e}_{ij}(t+\Delta t) - 2\,\Delta t\,\mu\,\lambda(t+\Delta t)\,S_{ij}(t+\Delta t)$$

$$+ \Delta t\,\mu\left[\lambda(t+\Delta t)S_{ij}(t+\Delta t) - \lambda(t)S_{ij}(t)\right] \quad (2.42)$$

Because all terms containing $S_{ij}(t+\Delta t)$ are linear, we may solve directly for the predicted deviatoric stress at the advanced time level via

$$S_{ij}(t+\Delta t) = \alpha\left[S^{e}_{ij}(t+\Delta t) - \Delta t\,\mu\lambda(t)S_{ij}(t)\right] \quad (2.43)$$

All terms on the right hand side of Equation (2.43) are known except for α. We determine α by requiring the $S_{ij}(t+\Delta t)$ to lie on the yield surface. As before we square Equation (2.43) and sum over i and j. Then

$$2K^2 = {}_{i,j}\Sigma\; S^2_{i,j}(t+\Delta t) = \alpha^2\,{}_{i,j}\Sigma\left[S^{e}_{i,j}(t+\Delta t) - (\Delta t)\mu\lambda(t)S_{ij}(t)\right]^2$$

Solving for α we obtain

$$\alpha = \frac{K}{\sqrt{1/2\,{}_{i,j}\Sigma\left[S^{e}_{ij}(t+\Delta t) - \Delta t\mu\lambda(t)S_{ij}(t)\right]^2}} \quad (2.44)$$

To sum up, the procedure for solving Equation (2.35) is given by the following three step algorithm:

i) Determine $S^{e}_{ij}(t+\Delta t)$ by solving Equation (2.35), by any second order method, with $\lambda = 0$.

ii) Test if $\Sigma\left[S^{e}_{ij}(t+\Delta t)\right]^2 < 2K^2$. If true, set $S_{ij}(t+\Delta t) = S^{e}_{ij}(t+\Delta t)$ otherwise determine α from Equation (2.44).

iii) Finally solve for the deviatoric stresses at the advanced time level using

$$S_{ij}(t+\Delta t) = \alpha\left[S^{e}_{ij}(t+\Delta t) - (\Delta t)\mu\lambda(t)S_{ij}(t)\right] \quad (2.45)$$

with

$$\lambda = (2K^2)^{-1}\;\Sigma\; S_{mn}(t)\,\dot{\varepsilon}_{mn}(t)$$

$$1 \leq m \leq 3$$
$$1 \leq n \leq 3$$

c) Final Form of the Differential Equations

It is now appropriate to describe the form of the differential equations used for the solution interior to the domain. Here we write the first four differential equations in conservation form choosing the entries of the vector w to be the quantities conserved across discontinuous transitions, i.e.,

$$w = \begin{pmatrix} \rho \\ \rho u \\ \rho v \\ E \end{pmatrix}$$

Here E is the sum of the specific internal and kinetic energy, the total energy, $E = \rho(e + 1/2(u^2 + v^2))$.

The continuity equation is

$$\rho_t + (\rho u)_x + (\rho v)_y = 0 \qquad (2.46)$$

The axial momentum equation is

$$(\rho u)_t + (\rho u^2 - \tau_{11})_x + (\rho uv - S_{12})_y = 0 \qquad (2.47)$$

The radial momentum equation is

$$(\rho v)_t + (\rho uv - S_{12})_x + (\rho v^2 - \tau_{22})_y = 0 \qquad (2.48)$$

Conservation of energy requires that E satisfy

$$E_t + \left[(E - \tau_{11})u - S_{12}v\right]_x + \left[(E - \tau_{22})v - S_{12}u\right]_y = 0 \qquad (2.49)$$

The stress strain relationships are not relationships that express a conservation principle. Hence they are rewritten here in their quasilinear component form:

$$S_{11,t} + uS_{11,x} + vS_{11,y} + \frac{2}{3}\mu(-2u_x + v_y) + S_{12}(v_x - u_y) = 0 \tag{2.50}$$

$$S_{12,t} + uS_{12,x} + vS_{12,y} - \mu(u_y + v_x) + \frac{S_{11}-S_{22}}{2}(u_y - v_x) = 0 \tag{2.51}$$

$$S_{22,t} + uS_{22,x} + vS_{22,y} + \frac{2\mu}{3}(-2v_y + u_x) + S_{12}(u_y - v_x) = 0 \tag{2.52}$$

In the next section we describe the difference scheme used.

III.

Finite Difference Equations

The partial differential equations described in Section III-C are partially in conservation form (2.46 - 2.49) and quasilinear form (2.50 - 2.52). This differential form is used to construct the difference scheme to be used at interior mesh points. This discussion concerns the difference scheme used, the two step method for the conservation form of the defining partial differential equations.

We wish to solve the set of equations defined in the previous section, Equations (2.46 - 2.52), on a set of mesh points

$$\begin{aligned} \alpha_i &= i\Delta\alpha \ , \ i = 0,1,\ldots,I \\ \beta_j &= j\Delta\beta \ , \ j = 0,1,\ldots,J \\ t_n &= n\Delta t \ , \ n = 0,1,\ldots \end{aligned} \tag{2.53}$$

Here we have introduced the coordinate transformation $\alpha = \alpha(x,y)$ and $\beta = \beta(y)$.

For convenience we introduce vector notation for the first four equations (2.46 - 2.49). Let f and g be four vectors defined by

$$f = \begin{pmatrix} \rho u \\ \rho u^2 - \tau_{11} \\ \rho uv - S_{12} \\ (E-\tau_{11})u - S_{12}v \end{pmatrix}, \quad g = \begin{pmatrix} \rho v \\ \rho uv - S_{12} \\ \rho v^2 - \tau_{22} \\ (E-\tau_{22})v - S_{12}u \end{pmatrix} \tag{2.54}$$

Then with $w^T = (\rho, \rho u, \rho v, E)$ we have

$$w_t + f_x + g_y = 0 \tag{2.55}$$

In the $\alpha - \beta$ plane (2.55) becomes, after application of the chain rule

$$w_t + f_\alpha + \alpha_y g_\alpha + \beta_y g_\beta = 0$$

or

$$\left(\frac{w}{\beta_y}\right)_t + \left(\frac{\tilde{f}}{\beta_y}\right)_\alpha + g_\beta = 0 \tag{2.56}$$

where $\tilde{f} = f + \alpha_y g$. For the remainder of the discussion we drop the tilda on f.

The numerical solution to (2.56) is called V;

$$V(\alpha_i,\beta_j,t_n) = V^n_{ij} \tilde{\approx} w(\alpha_i,\beta_j,t_n) \tag{2.57}$$

This approximate solution is written as a two step difference equation. Predicted values $\bar{V}$ are first obtained at the midpoints $(\alpha_{i+1/2},\beta_{j+1/2},t+n\Delta t)$ of the mesh by a first order difference approximation. These values are then used to obtain a second order accurate solution at regular mesh points. Letting $\lambda_1 = \Delta t/\Delta\alpha$ and $\lambda_2 = \Delta t/\Delta\beta$ the finite difference equation for the first step is

$$\begin{aligned}\bar{V}^{\,n}_{i+1/2,j+1/2} = 1/4\ (&V^{n-1}_{i+1,j+1} + V^{n-1}_{i+1,j} + V^{n-1}_{i,j+1} + V^{n-1}_{i,j}) \\ &- 1/2\lambda_1(f^{n-1}_{i+1,j+1} - f^{n-1}_{i,j+1} + f^{n-1}_{i+1,j} - f^{n-1}_{i,j}) \\ &- 1/2\lambda_2(g^{n-1}_{i+1,j+1} - g^{n-1}_{i+1,j} + g^{n-1}_{i,j+1} - g^{n-1}_{i,j})\end{aligned} \tag{2.58}$$

Introducing the notation $\bar{f}=f(\bar{V})$ the second step is defined by the finite difference equations

$$\begin{aligned}V^n_{i,j} = V^{n-1}_{i,j} &- 1/4\lambda_1(f^{n-1}_{i+1,j} - f^{n-1}_{i-1,j} + \bar{f}^n_{i+1/2,j+1/2} \\ &- \bar{f}^n_{i-1/2,j+1/2} + \bar{f}^n_{i+1/2,j-1/2} - \bar{f}^n_{i-1/2,j-1/2}) \\ &- 1/4\lambda_2(g^{n-1}_{i,j+1} - g^{n-1}_{i,j-1} + \bar{g}^n_{i+1/2,j+1/2} \\ &- \bar{g}^n_{i+1/2,j-1/2} + \bar{g}^n_{i-1/2,j+1/2} - \bar{g}^n_{i-1/2,j-1/2})\end{aligned} \tag{2.59}$$

Stability of the above difference scheme is achieved if an artificial viscosity Q is added to the right hand side of Equation (2.59)

$$Q = K\left\{\lambda_1\left[|\tilde{u}_{i+1,j} - \tilde{u}_{i,j}|\ (V_{i+1,j} - V_{i,j}) - |\tilde{u}_i - \tilde{u}_{i-1}|\ (V_{i,j} - V_{i-1,j})\right] + \lambda_2\left[|\tilde{v}_{i,j+1} - \tilde{v}_{i,j}|\ (V_{i,j+1} - V_{i,j}) - |\tilde{v}_{i,j} - \tilde{v}_{i,j-1}|\ (V_{i,j} - V_{i,j-1})\right]\right\} \tag{2.60}$$

where $\tilde{u}$ and $\tilde{v}$ are equal to $\hat{\alpha}$ and $\hat{\beta}$ respectively. The time step Δt is kept at approximately 2/3 of the maximum allowable CFL value, i.e., $\Delta t = .65\ \Delta t_{CFL}$. We compute the Courant-Friedrichs-Lewey time step by finding η,

$$\eta = \max_{i,j}\left\{(\tilde{u} + \sqrt{\alpha_y^2 + 1}\ C)/\Delta x,\ (\tilde{v} + \beta_y C)/\Delta y\right\}$$

over all mesh points. The maximum time step is then $\Delta t_{CFL} = 1/D\eta$.

Equations (2.50), (2.51) and (2.52) for the deviatoric stress components are solved in an analogous manner. Now let $\bar{w}^T = (S_{11}, S_{12}, S_{22})$, $s^T = (\rho, u, v, e, S_{11}, S_{12}, S_{22})$, and

$$f = \begin{pmatrix} -\frac{4}{3}\mu u \\ -\mu v \\ \frac{2}{3}\mu u \end{pmatrix} \text{ and } g = \begin{pmatrix} \frac{2}{3}\mu v \\ -\mu u \\ -\frac{4}{3}\mu v \end{pmatrix} \tag{2.61}$$

and define the matricies a and b as

$$a = \begin{pmatrix} 0 & 0 & S_{12} & 0 & u & 0 & 0 \\ 0 & 0 & -\frac{S_{11}-S_{22}}{2} & 0 & 0 & u & 0 \\ 0 & 0 & -S_{12} & 0 & 0 & 0 & u \end{pmatrix} \tag{2.62}$$

and

$$b = \begin{pmatrix} 0 & -S_{12} & 0 & 0 & v & 0 & 0 \\ 0 & \frac{S_{11}-S_{22}}{2} & 0 & 0 & 0 & v & 0 \\ 0 & S_{12} & 0 & 0 & 0 & 0 & v \end{pmatrix}$$

Then introduce two transform matricies A and B given in terms of a and b, $A = a + (a+\alpha_y b)/\beta_y$ and B=B. In vector notation the form used to generate the difference scheme, in terms of the above matrices, with $\hat{f} = (f + \alpha_y g)/\beta_y$ is just

$$\left(\frac{\bar{w}}{\beta_y} \right)_t + f_\alpha + g_\beta + Aw_\alpha + Bw_\beta = 0 \qquad (2.63)$$

If the terms with coefficients in Equation (2.63) when put into difference form are centered, the same two step algorithm (2.58) and (2.59) results for the stress deviators $\bar{w}$.

The above difference scheme, in order to be applied at all interior points of the mesh (2.53) requires the definition of dependent variables at all lattice points of the finite difference mesh. For interior points which do not have all nearest neighbors the following scheme is used.

The four nearest neighbors are checked first. If any of these points are missing, values of the dependent variables are extrapolated at the missing point from data at the central lattice point and the boundary crossing between this point and the missing point. The four corner points are then checked. If one of these points is missing, values of the dependent variables are extrapolated using data at the three points that are in the same quadrant of the lattice as the missing point. These points are either interior or have already been defined by extrapolation. In the figure shown the dependent variables at point 2 are obtained by linear extrapolation from values at interior point 1 and boundary point A. Values at point 3 are obtained by first interpolating values of dependent variables at point B from values at points 2 and 4 and then extrapolating values from points 1 and B. In this way, the regular two step difference scheme can be used for all interior points except for points lying within Δ of the boundary (see reference 1).

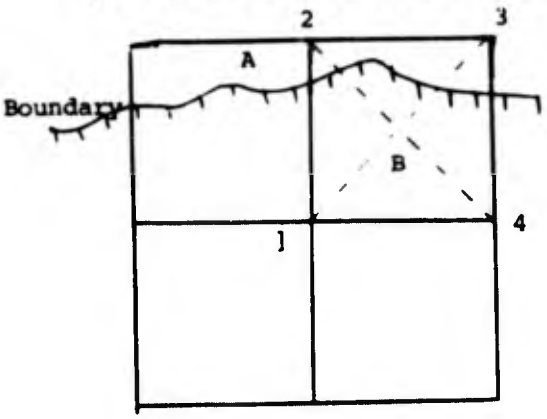

IV. RESULTS

In order to demonstrate the versatility of the algorithm, two problems were considered. Each material in both problems is assumed to have an equation of state which is given by Tillotson:

Compressed states: $p=p_c$

$$p_c = \left(a + \frac{b}{\frac{E}{E_0\eta^2}+1}\right)E\rho + A\xi + B\xi^2, \quad \rho > \rho_0 \ , \ 0 < E < E_s$$

where $\xi = \eta - 1$, $\eta = \rho/\rho_0$

Expanded States: $p=p_e$

$$p_e = aE\rho + \left(\frac{bE\rho}{\frac{E}{E_0\eta^2}+1} + A\xi e^{-\tau\left(\frac{1}{\eta}-1\right)}\right) e^{-\alpha\left(\frac{1}{\eta}-1\right)^2} \ , \ \rho < \rho_0, \quad E > E_s$$

Intermediate States:

$$p = \frac{(E - E_s)p_e + (E'_s - E)p_c}{E'_s - E_s} \qquad \rho < \rho_0 \ , \ E_s < E < E'_s$$

The constants used in the above equation of state for the present calculation are given in the following table.

TILLOTSON CONSTANTS

	ρ_0	a	b	A	B	α	β	E_0	E_s	E'_s	μ	Y_c
	gm/cm^3			10^{12}dynes/cm^2	10^{12}dynes/cm^2			10^{12}ergs/gm	10^{12}ergs/gm	10^{12}ergs/gm	10^{12}dynes/cm^2	10^{12} dynes/cm^2
90-25 Tungsten Alloy	17.04	0.5	1.04	3.08	2.5	10.	10.	0.225	0.0111	0.056	1.2967	0.0111
RHA	7.8	0.5	1.50	1.28	1.05	5.	5.	0.095	0.0244	0.102	0.8077	0.01219
Maraging 300	8.0	0.5	1.50	1.28	1.05	5.	5.	0.095	0.0244	0.102	0.796	0.0192

The coefficient of viscosity K in Equation (2.60) was taken to be 0.0. The transformation

$$\alpha = D(z-mr) \quad , \frac{1}{m} = \tan \omega$$

where ω = angle of attack measured from the x-axis, is used in the projectile. There is no β transformation used in the projectile and no transformation in α and β used in the target. The constants for the transformations applied to each material domain are given in the accompanying table.

TRANSFORMATION CONSTANTS

	D	ω
90/25 Tungsten	Δz^{-1}	65°
RHA	Δz^{-1}	90°
Maraging-300	Δz^{-1}	65°

The mesh $(i\Delta\alpha, j\Delta\beta)$, which was chosen such that $1 \leq i \leq I$, $1 \leq j \leq J$, is given in the following table for each of the domains.

There were two problems considered for each of the two cases described below:

Case 1: Silver Bullet, ω=65° and U_∞=.0186$\frac{cm}{\mu sec.}$ target thickness = 0.9525 cm. (2.54 cm.)

Case 2: Round nose sheathed, ω=65° and U_∞=.0234$\frac{cm}{\mu sec.}$ target thickness = 0.9525 cm. (2.54 cm.)

MESH CONSTANTS

	I	J	i_0-right	j_0-top	j_0-bottom	i_0-left	Δz cm	Δr cm
90/25 Tungsten	15 (15)	35 (35)	12 (12)	34 (34)	2 (2)	3 (3)	.33 (.275)	.14 (.98)
RHA	17 (14)	140 (140)	15 (12)	139 (139)	2 (2)	10 (7)	.16 (.16)	.58 (.58)
Maraging-300	36 (40)	15 (15)	32 (32)	14 (14)	2 (2)	3 (3)	12 (.09)	2.43 (3.18)

Note: Case 2 data is represented by () in the above table.

Here i_0 and j_0 represent respectively the initial α position of the material right justified on the mesh and the initial maximum height of the material in the β direction. The initial starting value of i_0 left justified is also shown and the minimum value of j_0 is also shown.

The initial velocity components as used in Case 1: (-.05781, -.124); Case 2: (-.0647, -.1388).

Figure 1 shows the configuration of projectile and target at the moment of impact for case 1. Figure 2 is a blow-up of the interaction region. After slightly more than 20 μ-sec. the projectile has essentially perforated the target; this is shown in Figure 3. The plastic flow regions are indicated by "P" at the mesh points which satisfy (2.39). A blow-up of this interaction region is shown in Figure 4. Due to the thin target, projectile damage is predictably small - essentially limited to a slight degree of blunting on the upper projectile surface at the ogive. The computation was allowed to proceed until slightly greater than 25μsec. elapsed, as shown in Figure 5. The back face of the target is moving out rapidly at this late stage but there is no further enhancement of damage to the projectile.

For comparison, an identical computation was run with a target which was 2.54 cm. thick compared to the .95 cm. target described above. As would be expected, the damage imparted to the projectile indicates the beginning of a significant level of upper body distortion on the forward end of the projectile. Some binding is noted by observing deflection of the lower edge of the forward portion of the projectile. This is seen in Figure 6 with a blow-up of the interaction region shown in Figure 7.

For the second case the geometrical configuration is shown at the moment of impact in Figure 8. In Figure 9 we see the complete configuration after slightly more than 20μsec. with a blow-up of the interaction region in Figure 10. The plastic wave travel in the core of the projectile is a numerical artifice and is directly controllable by requiring that the ratio of mesh increments $\Delta x/\Delta y$ be on the order of less than 3 to 1. It was a difficult ratio to achieve in this calculation due to the fine resolution required in the sheath of the projectile. Future modifications to SMITE will allow greater flexibility in allocation of memory space so that such resolution requirements will not be a future problem.

To compare this calculation, in a similar manner to that carried out in the first problem, a second computation in which the same materials were used, including precisely the same projectile, but a target of 2.54 cm. thickness, rather than a target thickness of .95 cm. which was used in the above problem. After slightly more than 20μsec., shown in Figure 11, with a blow-up of the interaction region shown in Figure 12, we see rather severe distortions of the frontal region of the projectile. A large degree of downward bending is apparent with indications that the projectile core is starting to leave the forward edge of the top of the sheath. At this point in time the target is still holding up well. To determine a better appraisel of the extent of projectile distortion, the computation would have to be carried out for at least another 20μsec.

Figure 1

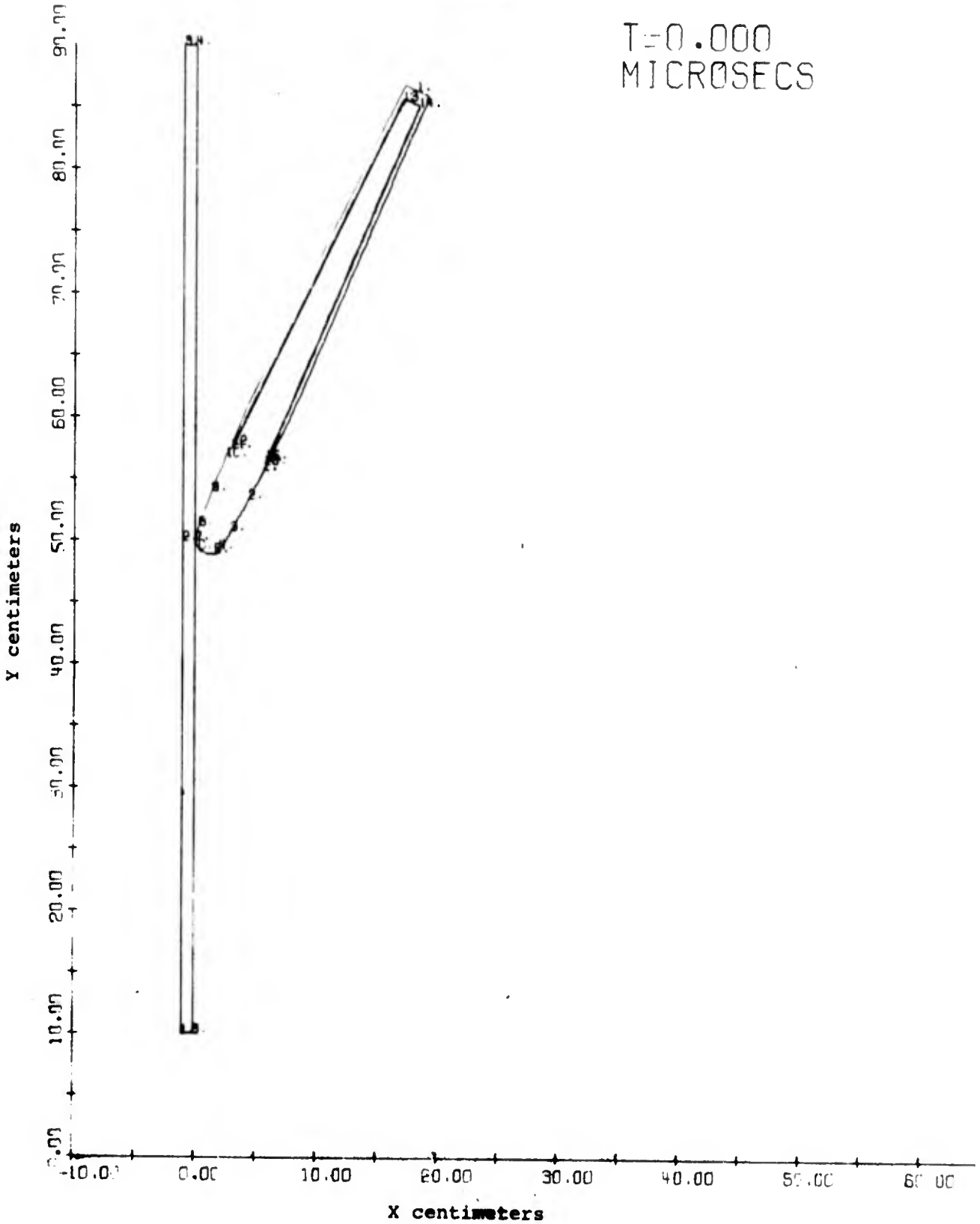
T=0.000
MICROSECS
Y centimeters
X centimeters
90.00
80.00
70.00
60.00
50.00
40.00
30.00
20.00
10.00
0.00
-10.00
0.00
10.00
20.00
30.00
40.00
50.00
60.00

Figure 2

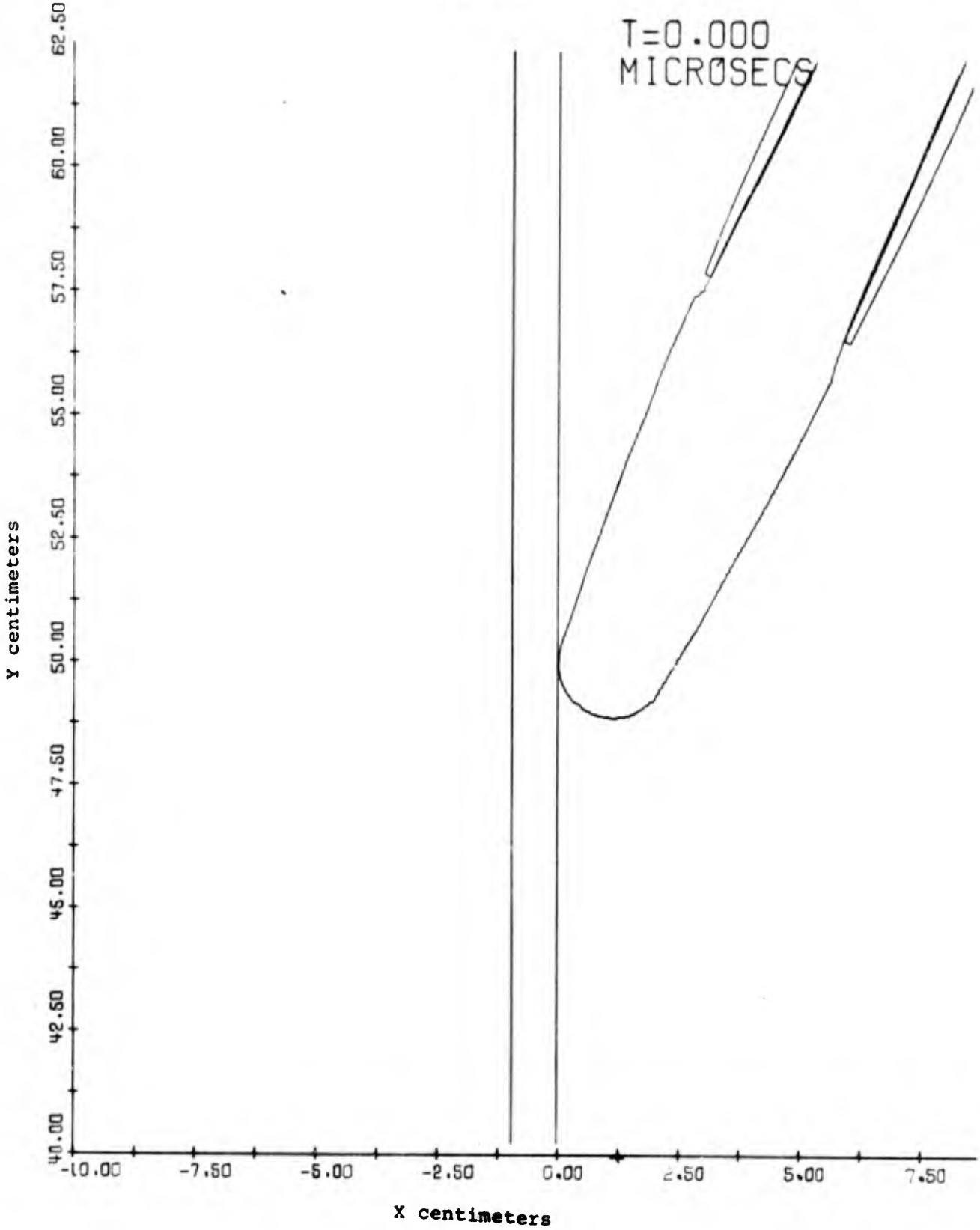
T=0.000
MICROSECS
62.50
60.00
57.50
55.00
52.50
50.00
47.50
45.00
42.50
40.00
-10.00
-7.50
-5.00
-2.50
0.00
2.50
5.00
7.50
Y centimeters
X centimeters

Figure 3

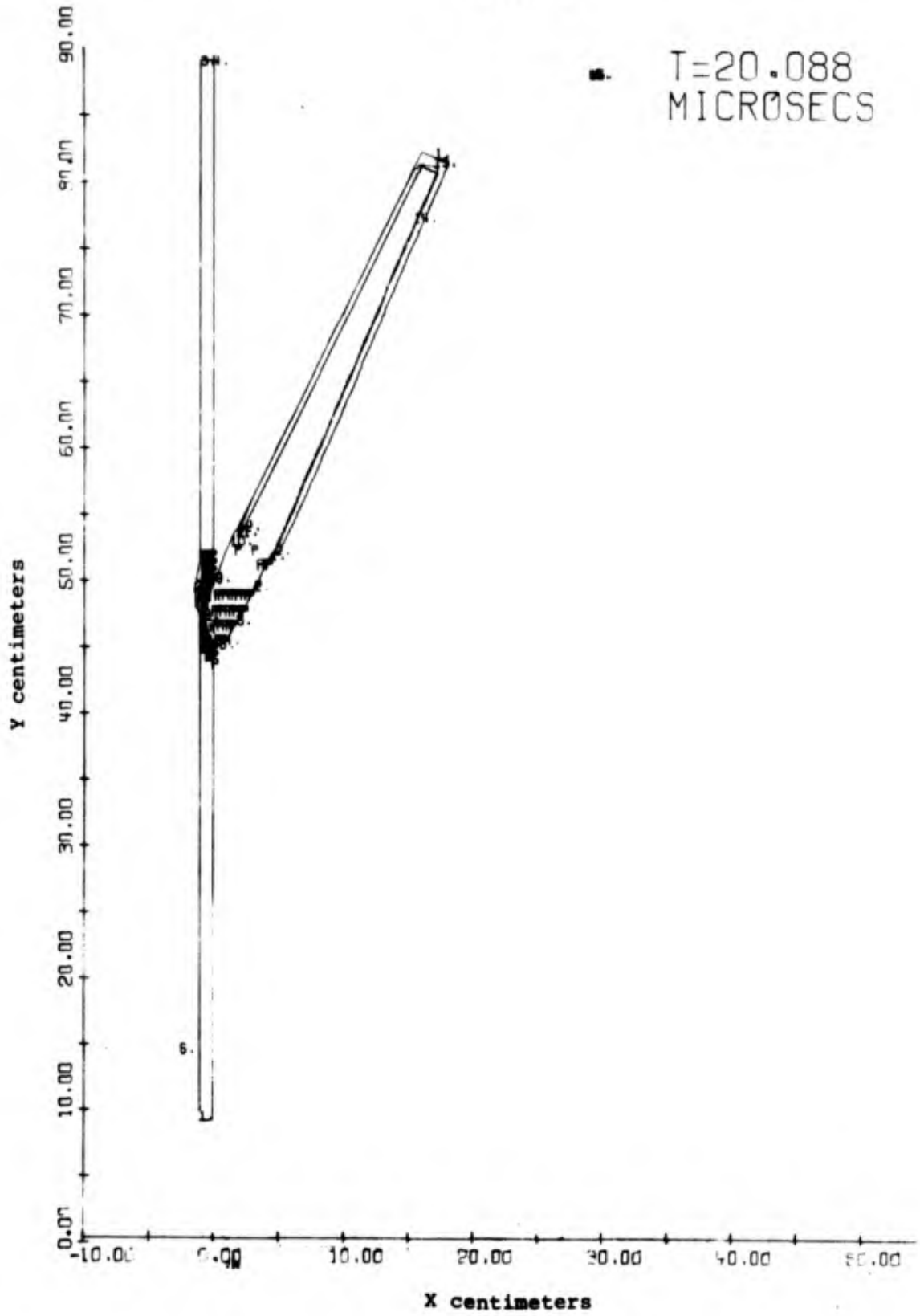
T=20.088
MICROSECS
Y centimeters
X centimeters
90.00
70.00
60.00
50.00
40.00
30.00
20.00
10.00
0.00
-10.00
0.00
10.00
20.00
30.00
40.00

Figure 4

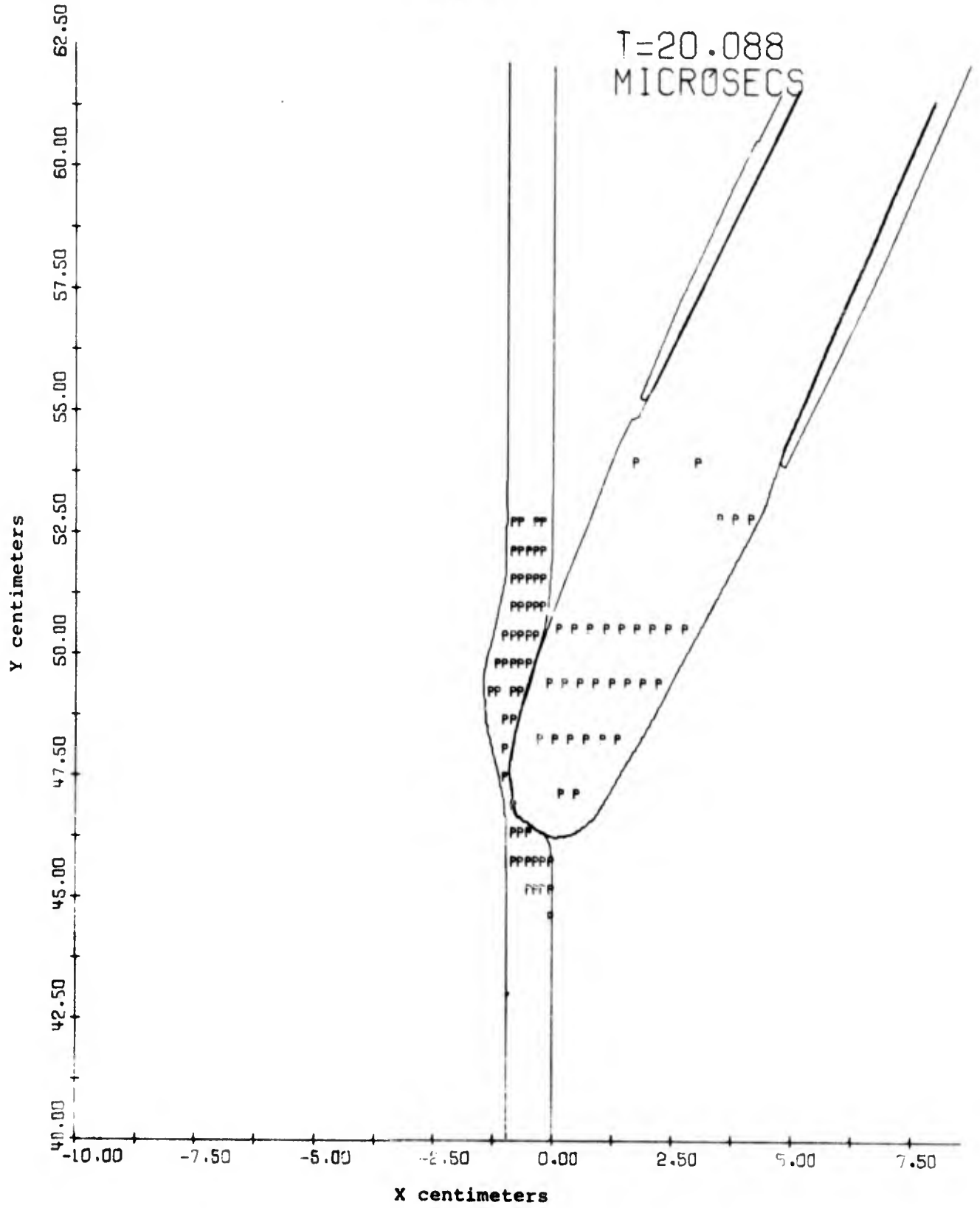
T=20.088
MICROSECS
Y centimeters
62.50
60.00
57.50
55.00
52.50
50.00
47.50
45.00
42.50
40.00
-10.00
-7.50
-5.00
-2.50
0.00
2.50
5.00
7.50
X centimeters

Figure 5

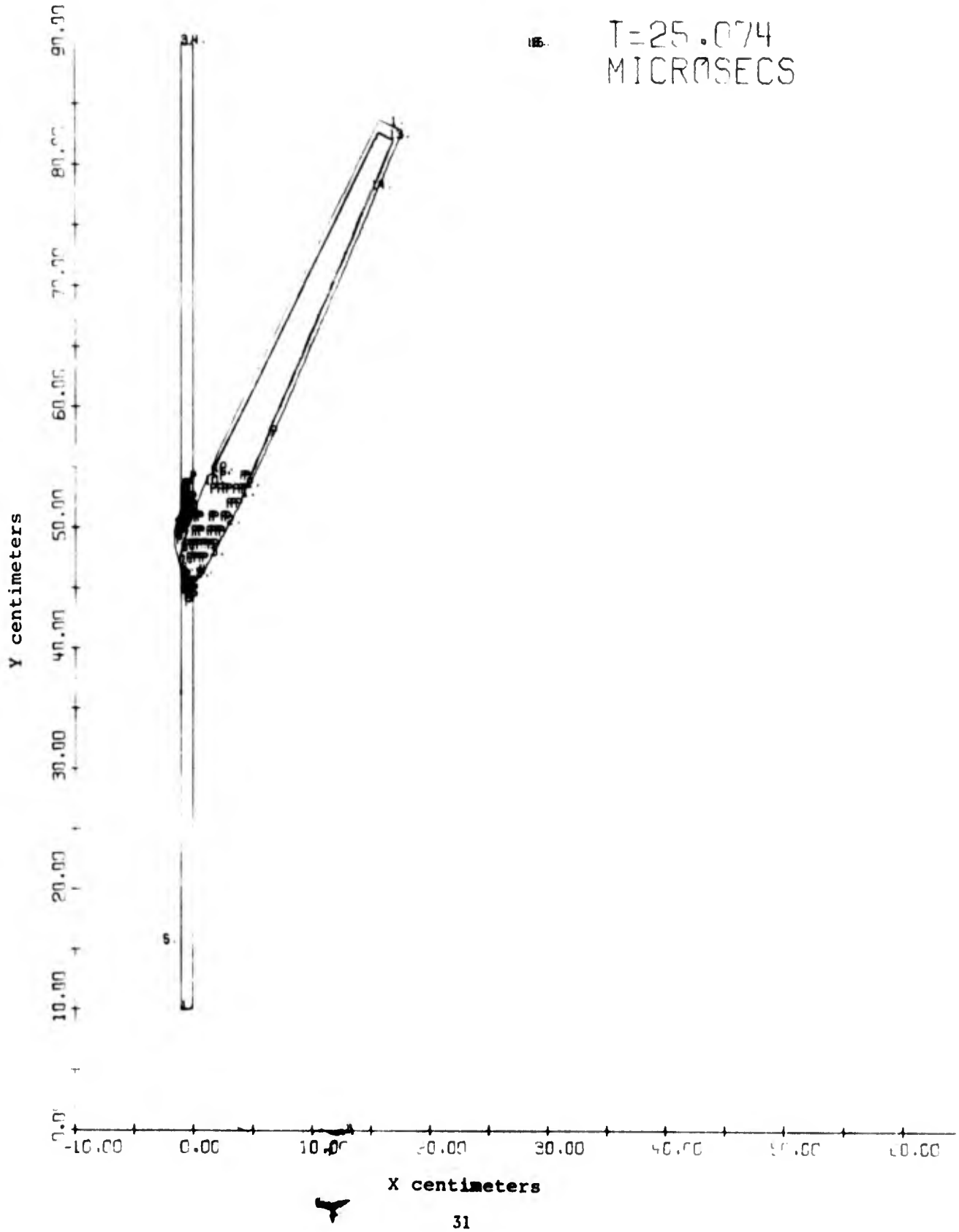
T=25.074
MICROSECS
Y centimeters
X centimeters
-10.00
0.00
10.00
30.00
90.00
80.00
70.00
60.00
50.00
40.00
30.00
20.00
10.00
0.0

Figure 6

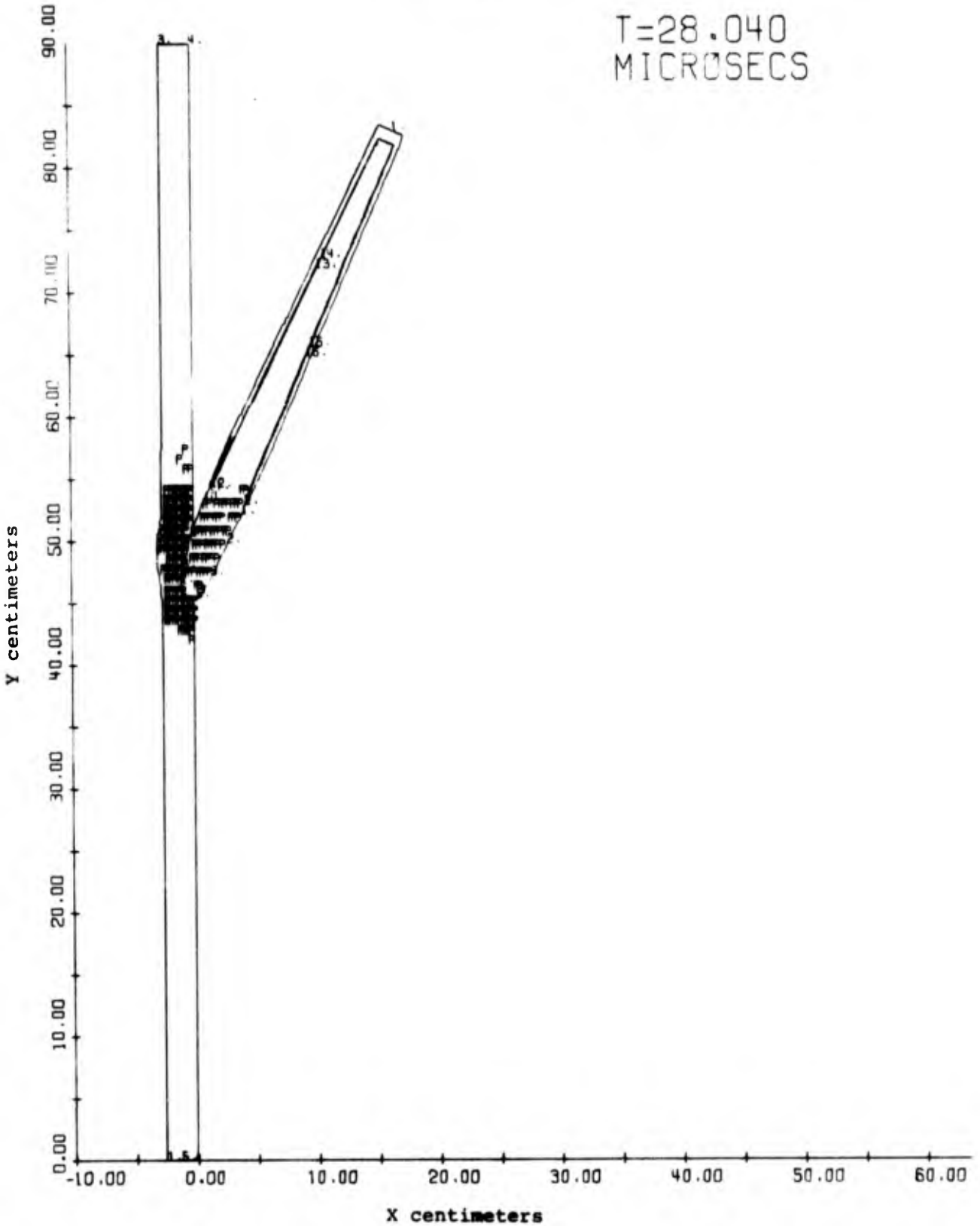
T=28.040
MICROSECS
Y centimeters
X centimeters
90.00
80.00
70.00
60.00
50.00
40.00
30.00
20.00
10.00
0.00
-10.00
0.00
10.00
20.00
30.00
40.00
50.00
60.00

Figure 7

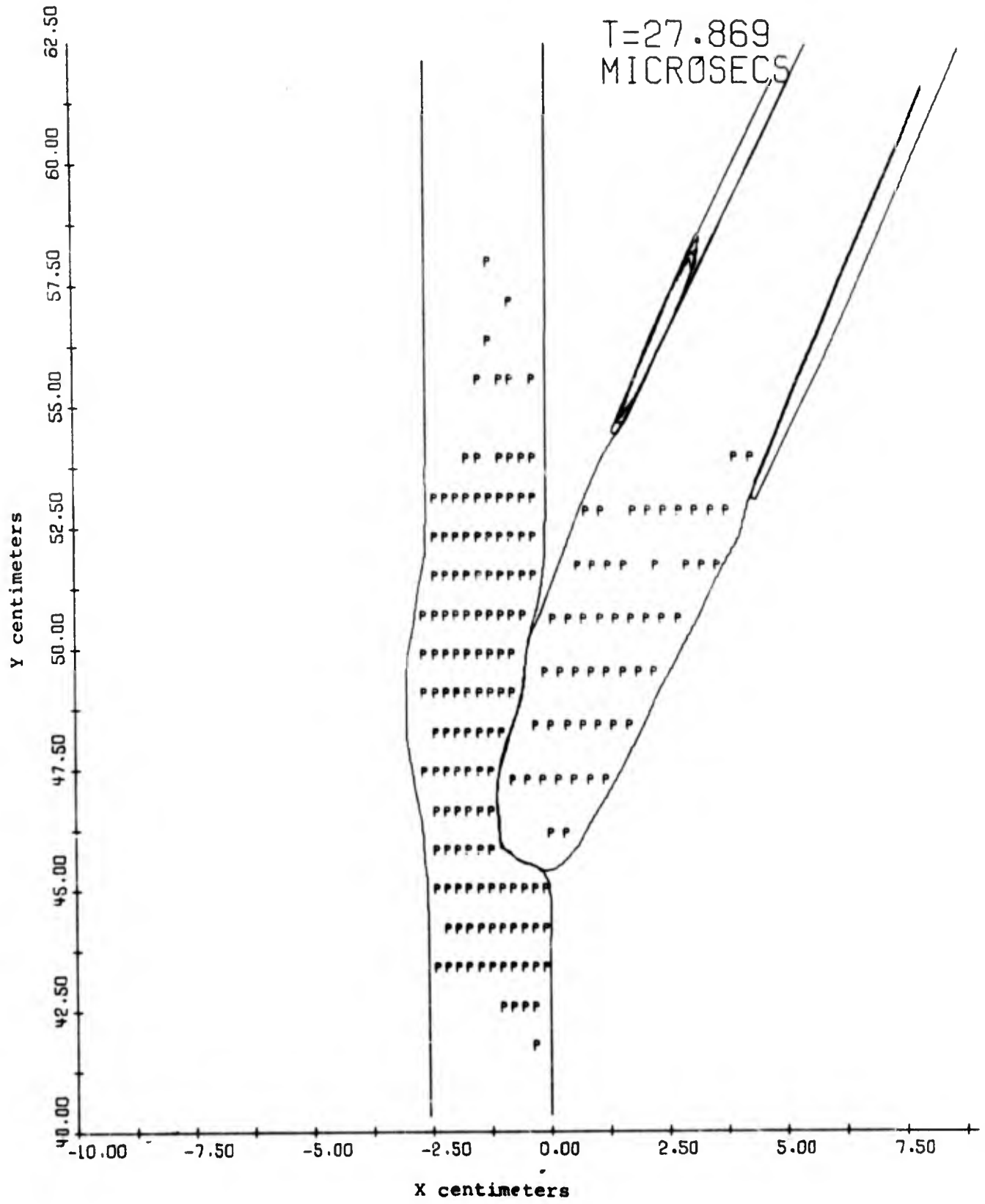
T=27.869
MICROSECS
Y centimeters
62.50
60.00
57.50
55.00
52.50
50.00
47.50
45.00
42.50
40.00
-10.00
-7.50
-5.00
-2.50
0.00
2.50
5.00
7.50
X centimeters

Figure 8

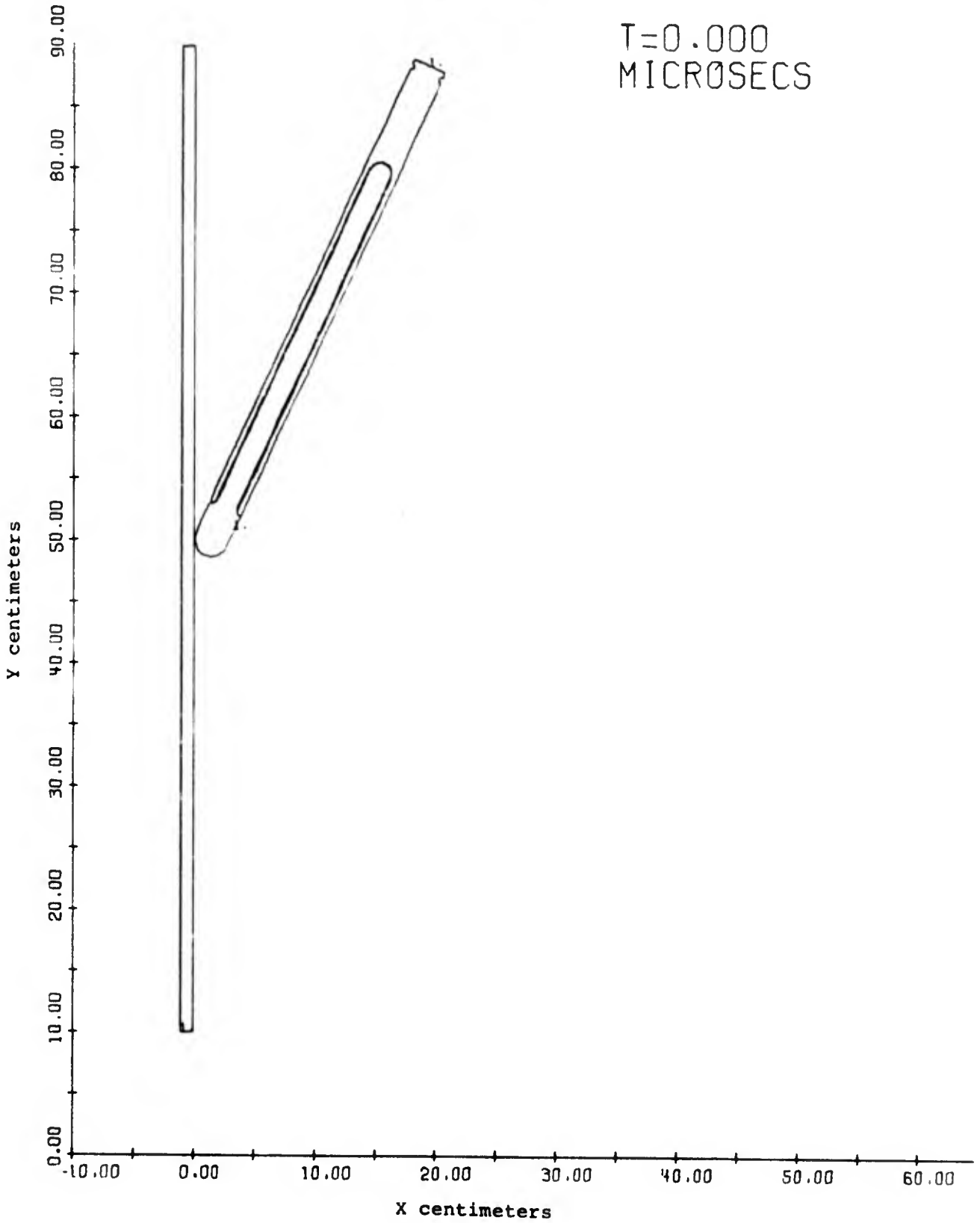
T=0.000
MICROSECS
Y centimeters
X centimeters
0.00
10.00
20.00
30.00
40.00
50.00
60.00
70.00
80.00
90.00
-10.00
0.00
10.00
20.00
30.00
40.00
50.00
60.00

Figure 9

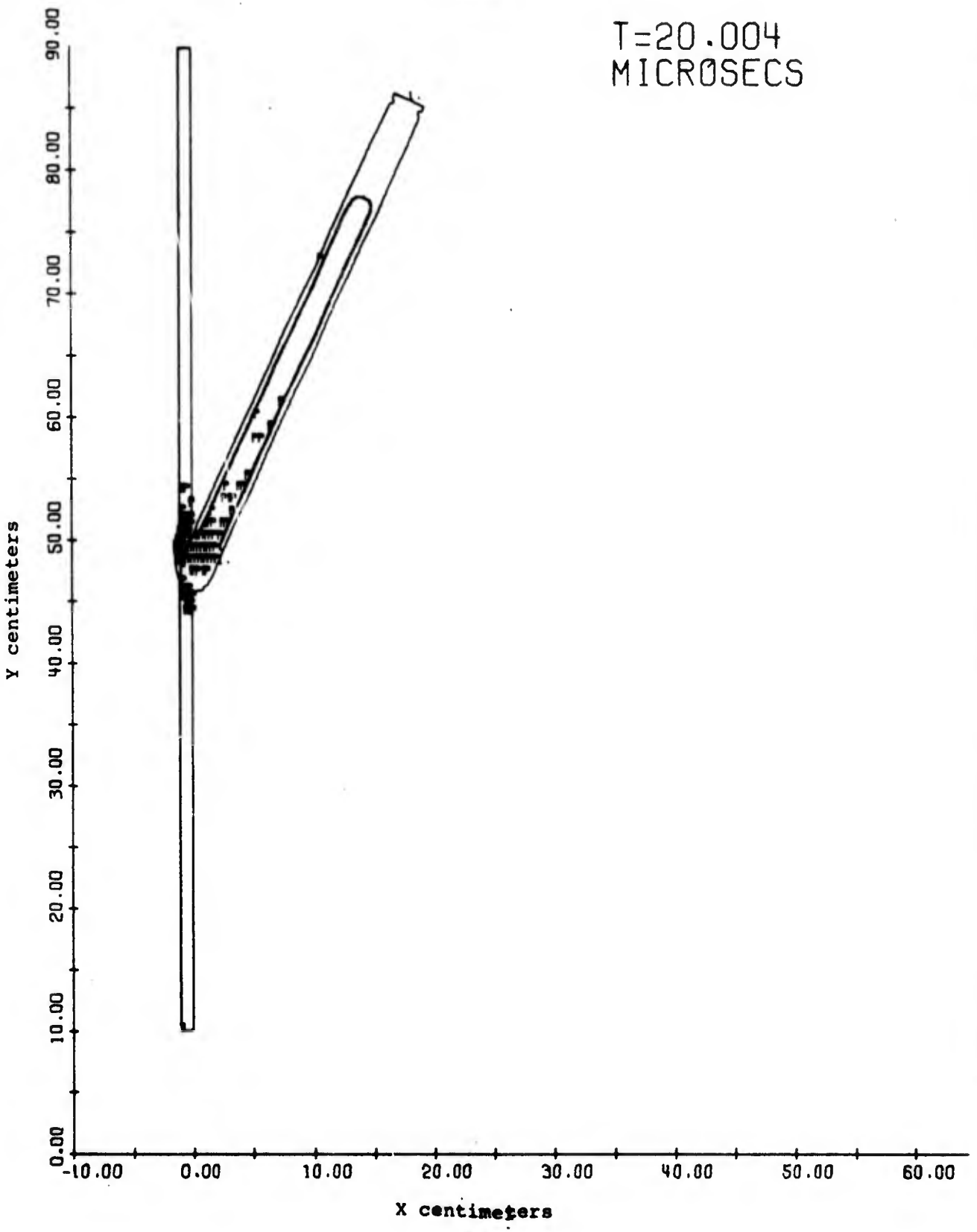
T=20.004
MICROSECS
Y centimeters
90.00
80.00
70.00
60.00
50.00
40.00
30.00
20.00
10.00
0.00
-10.00
0.00
10.00
20.00
30.00
40.00
50.00
60.00
X centimeters

Figure 10

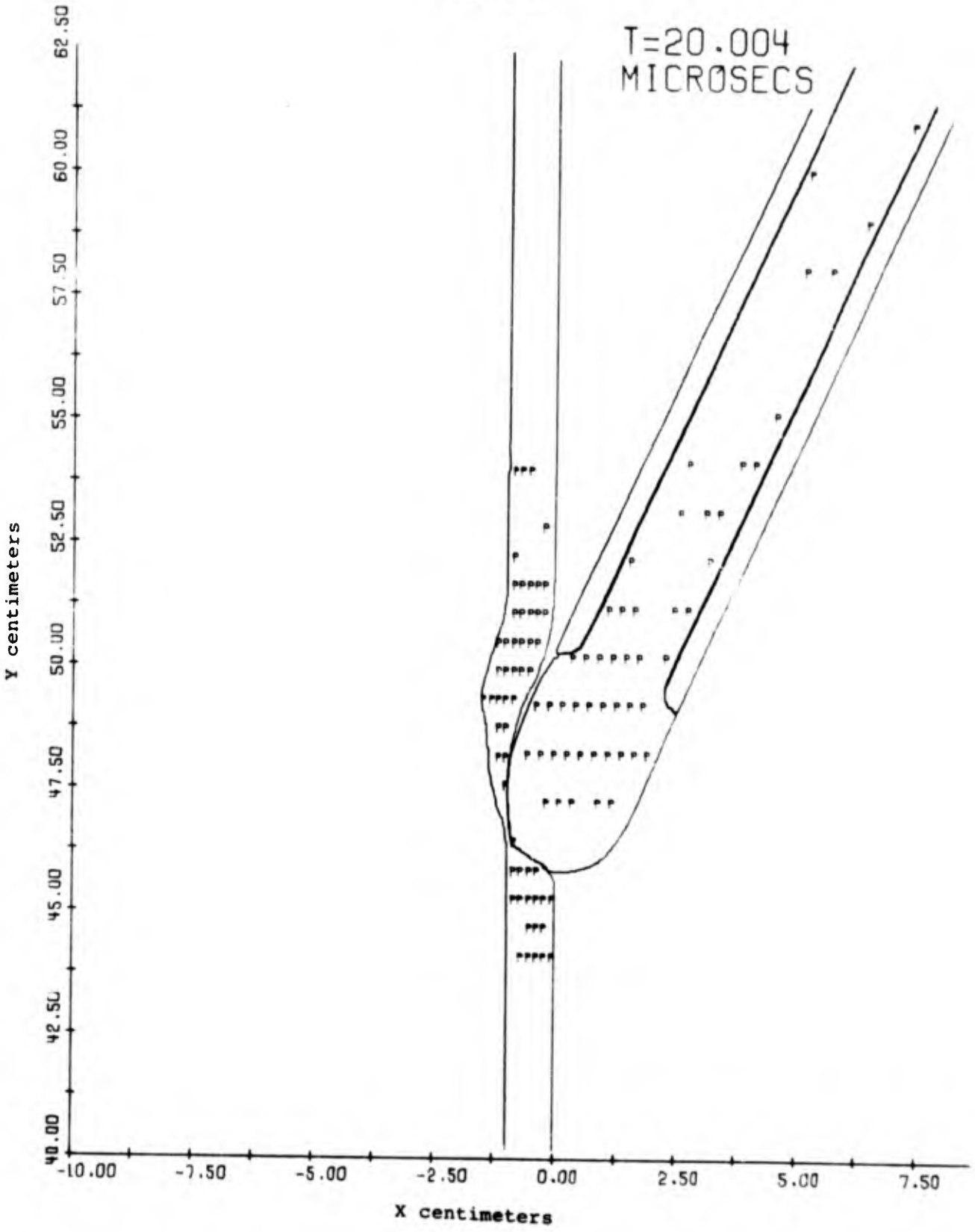
T=20.004
MICROSECS
62.50
60.00
57.50
55.00
52.50
50.00
47.50
45.00
42.50
40.00
Y centimeters
-10.00
-7.50
-5.00
-2.50
0.00
2.50
5.00
7.50
X centimeters

Figure 11

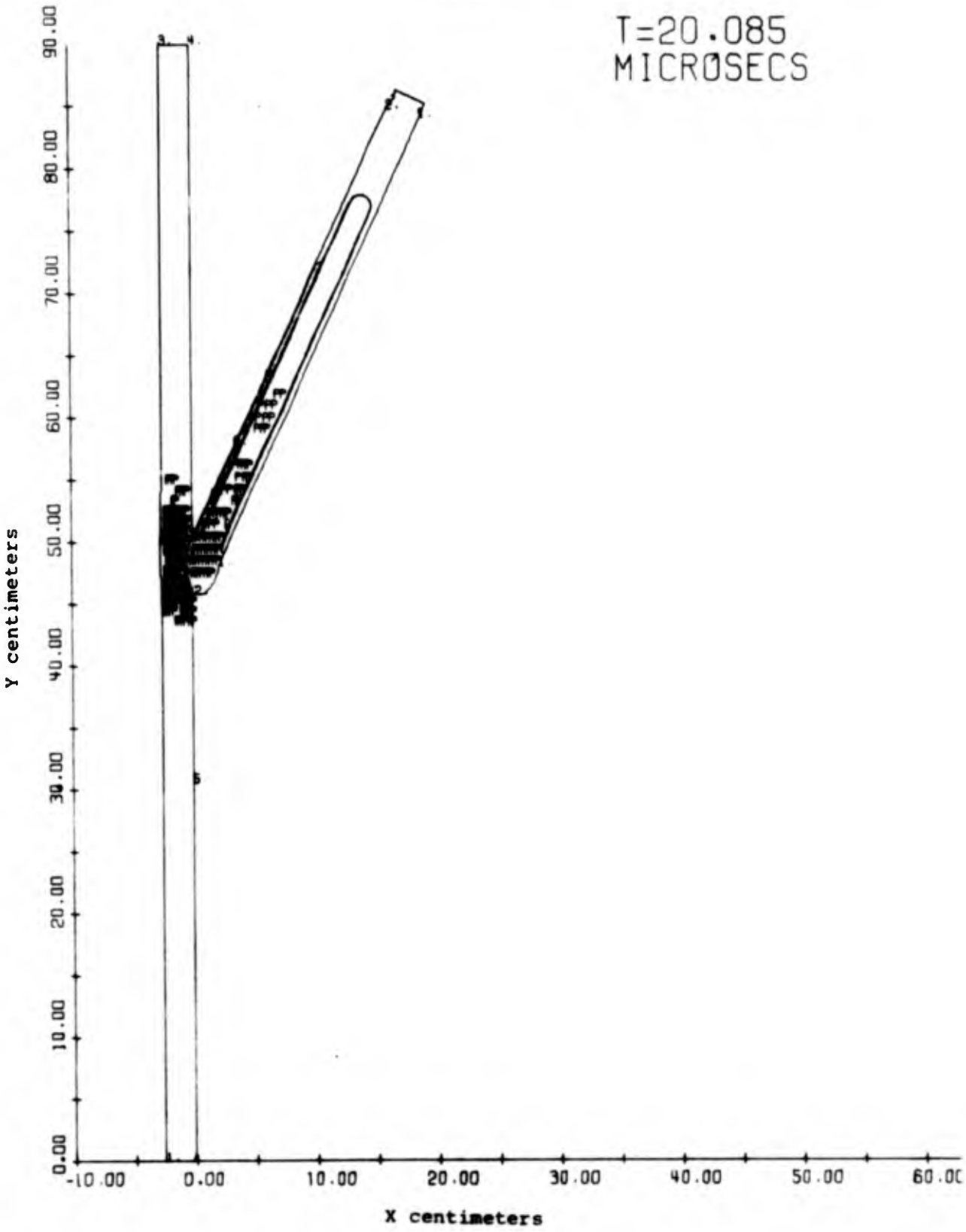
T=20.085
MICROSECS
Y centimeters
X centimeters
0.00
10.00
20.00
30.00
40.00
50.00
60.00
70.00
80.00
90.00
-10.00
0.00
10.00
20.00
30.00
40.00
50.00
60.00

Figure 12

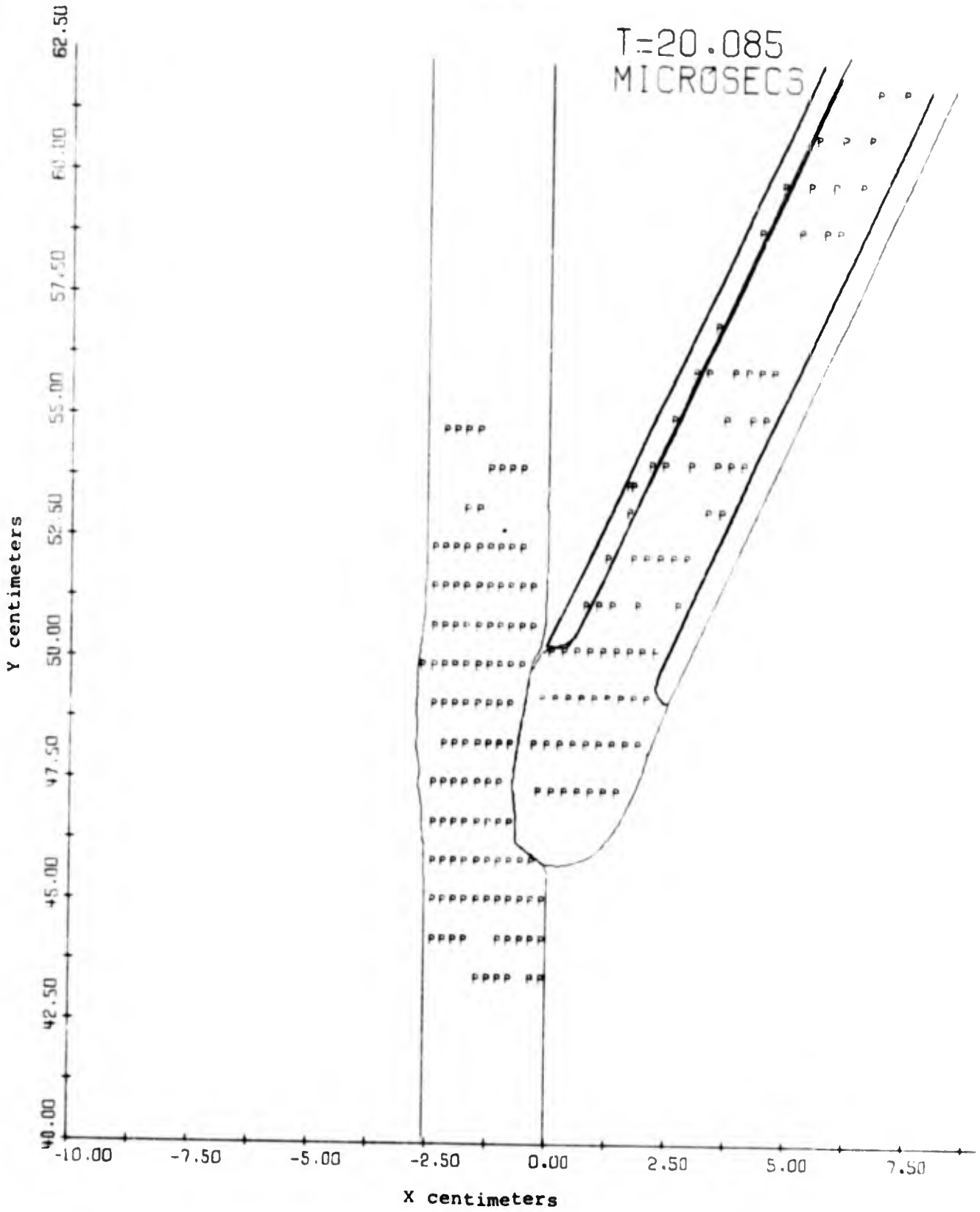
T=20.085
MICROSECS
62.50
57.50
52.50
50.00
47.50
45.00
42.50
40.00
-10.00
-7.50
-5.00
-2.50
0.00
2.50
5.00
7.50
Y centimeters
X centimeters

APPENDIX 1

Modifications to the input data deck for the SMITE Code for plane strain.

Input cards 2 and 3 have been changed. These cards should now read as follows:

CARD	COLS.	TYPE	NAME	DESCRIPTION
2	1-10	R	TMAX	Maximum problem time in microseconds.
	11-20	R	TPRIN	Print output increment in microseconds.
	21-30	R	TPRPL	Printer plot output increment in microseconds.
	31-40	R	TPLOT	Plot tape output increment in microseconds.
	41-50	R	TSAVE	Restart output increment in microseconds. If any output increment is negative that output is suppressed.
	51-60	R	TCOMP	Maximum computation time in seconds.
3	1-10	R	RDIS	Maximum fractional mesh allowed. If a point is closer to the boundary than this fraction of mesh size, interpolation will be used.
	11-20	R	PSCL	Scale of printer plot in centimeters per inch.
	21-30	R	XORG	Value in centimeters corresponding to left side of printer plot.
	31-40	R	YORG	Value in centimeters corresponding to bottom of printer plot.

APPENDIX 2

Sample of input data deck for the two cases (thin target) discussed in this report.

INPUT FOR CASE 1

```
 S=b  65D
40,0          10.0          2.5          2.5          1.0          2000.0
0.5           5,0          -20,0         40,0
     3     0
     2
     2    27    27     1     5     5     3    14    18     2    46    43
    17   140    10    15     2   139     3     2     4   600     1     1    99    99
0.9525       80.0          89.9         1600,0        80.0         0,0          0,0          0.65
0.8077       0.01219       7.80         0,0           0.0
•0.9525      10,0          -0,9525      50,0          -0.9525      90.0
•0.9525      90,0          0.0          90,0
0.0          90.0          0.0          50,0          0,0          10.0         -0,9525      10.0
     1     2     3     4     6
    15    35     3    12     2    34    41     5     5   200     1     2    99    99
3.30         37,0          65,0          1,0     E-6   37.0         0,0          0,0          0.65
1.2967       0,0111        17.04         -,05781       -0.124
    5,57880   55,71114      5,91687   55,87465      5.06735   54,71385      4,71328   54.05517
    4,35465   53,39862      3,29147   52,74419      3.62372   52,09189      3,25140   51.44172
    2,87450   50,79369      2,99302   50,14786      2.10693   49.50405      2,04950   49.40920
    2,98773   49,31637      1,91531   49,22851      1.83134   49.14603      1,73431   49.06965
    1,64175   49,01050      1,48939   48,94059      1.32876   48.89386      1,11822   48.87041
     ,63014   48,97357       ,24724   49,27655       .12987   49.45291       ,06242   49.60600
     ,02323   49,74510       ,00385   49,87657      0.00000   50.00000       ,00920   50.11734
     ,02995   50,22930       ,05135   50,33628       .09710   50.44125       ,34207   51.15080
     ,58164   51,85821       ,04580   52,56347      1.10453   53.26661      1,36784   53.96761
    1,63571   54,66648      1,90814   55,36323      2.18512   56.05785      2,46665   56.75036
    2,77486   57,43039
    2,77486   57,43039      2,77000   57,38605      3.09675   57.84084     17,05525   85.83725
   18,32136   85,24615
   18,32136   85,24685      5,94721   56,55828      5.64458   56.09225      5,74072   56.04742
    5,57880   55,71114
     1     5     3    13    17    22    27    32    36    40    42    43    44    45    46    47
    56    15     3    32     2    14    13     7    13   200     1     3    99    99
3.50         30,4          65,0          1,0     E-6   30.4         0,0          0,0          0.65
0.795        0,0192        8.00          -,05761       -0.124
   18,13768   30,46246     19,08614   86,01126      7.96774   60.55525      7,77995   60.14610
    7,50249   59,73773      7,38738   59,33014      7.19061   58.92331      6,99218   58.51727
    6,79209   58,11199      6,79034   57,70749      4.38692   57.30376      6,18185   56.90081
    5,97512   56,49863
    5,97512   56,49863      5,94721   56,55828     18.32136   85.24685     17,68830   85.54205
   17,05525   85,83725      3,09675   57,84084      2.96884   57.90046
    2,96884   57,90048      3,04404   58,31736      3.32090   58.73347      3,49943   59.14880
    3,67961   59,56336      3,86145   59,97715      4.04496   60.39016      4,23012   60.80239
    4,41694   61,21386      4,60542   61,62454      4.79556   62.03446     17,14922   86.91446
   18,11768   86,46286
     1
```

Preceding page blank

INPUT FOR CASE 2

```
CASE 2 65D
40.0        10.0        2.5         2.5         1.0         2000.0
0.5         5.0         -20.0       40.0
     3      0
     2
     2    21    21     1     5     5     3     9    51     2    63    23
    14   140     7    12     2   139     3     2     4   700     1     1    99    99
0.9525      80.0        89.9        1000.0      20.0        0.0         0.0         0.65
0.8077      0.01219     7.80        0.0         0.0
*0.9525     10.0        -0.9525     50.0        -0.9525     90.0
*0.9525     90.0        0.0         90.0
0.0         90.0        0.0         50.0        0.0         10.0        -0.9523     10.0
     1     2     3     4     6
    15    35     7    12     2    34    33    33     2   200     1     2    99    99
2.743       32.0        65.0        1.0         E-6 32.0        0.0         0.0         0.65
1.2967      0.0111      17.04       -.0047      -0.1388
    3.30259   50.91645    2.91435   49.44053    2.23740   48.95668    2.01798   48.81065
    1.82752   48.72674    1.65346   48.67798    1.49089   48.65387    1.33732   48.64907
    1.19133   48.66052    1.05204   48.68634     .91894   48.72542     .79173   48.77715
     .67034   48.84134     .55484   48.91819     .44553   49.00829     .34292   49.11277
     .24786   49.23349     .16135   49.37382     .08732   49.53821     .02918   49.73805
    0.00000   50.00000     .02835   50.29977    1.28527   53.08079    1.32605   53.06420
    1.36073   53.05167    1.41339   53.04339    1.46020   53.03973    1.50944   53.04126
    1.56157   53.04899    1.61738   53.06463    1.67845   53.09153    1.74880   53.13835
    1.86966   53.29349
    1.86966   53.29349   14.35290   80.14966   14.64899   80.47837   14.79805   80.57758
   14.92745   80.63459   15.04570   80.66771   15.15614   80.68409   15.26047   80.68735
   15.35965   80.67957   15.45428   80.66203   15.54471   80.63548   15.63113   80.60034
   15.71360   80.55673   15.79206   80.50452   15.86632   80.44331   15.93603   80.37233
   16.00060   80.29031   16.05904   80.19518   16.10968   80.08330   16.14918   79.94754
   16.16900   79.76958   16.18180   79.56211    3.55657   52.50594    3.51741   52.31364
    3.52677   52.22965    3.54541   52.16557    3.56931   52.11277    3.59689   52.06787
    3.62737   52.02916    3.66027   51.99566    3.69532   51.96677    3.73235   51.94213
    3.77127   51.92155
    3.77127   51.92155    3.80259   51.91645
     1     8    15    21    27    35    43
     4     15     3    32     2    14     9    43     7   300     1     3    99    99
2.743       39.772      65.0        1.0         E-6 39.772      0.0         0.0         0.65
0.796       0.0192      8.00        -.0647      -0.1388
   19.33664   88.54684   20.27964   87.90722   20.36495   87.50682   20.10031   87.63022
   19.96423   87.33839   20.42897   87.21499   14.71328   75.38676    8.37401   61.79215
    3.77127   51.92155
    3.77127   51.92155    3.74235   51.94213    3.69532   51.96677    3.66027   51.99566
    3.62737   52.02916    3.59689   52.06787    3.56931   52.11277    3.54541   52.16557
    3.52677   52.22965    3.51741   52.31364    3.55857   52.50594   16.08180   79.36211
   16.10900   79.76958   16.14918   79.94754   16.10968   80.08330   16.05904   80.19518
   16.00060   80.29031   15.93603   80.37233   15.86632   80.44331   15.79206   80.50452
   15.71360   80.55673   15.63113   80.60034   15.54471   80.63548   15.45428   80.66203
   15.35965   80.67957   15.26047   80.68735   15.15614   80.68409   15.04570   80.66771
   14.92745   80.63459   14.79805   80.57758   14.64899   80.47837   14.39290   80.14966
    1.86966   53.29349    1.74880   53.13835    1.67845   53.09153    1.61738   53.06463
    1.56157   53.04899    1.50944   53.04126    1.46020   53.03973    1.41339   53.04339
    1.36073   53.05167    1.32605   53.06420    1.28527   53.08079
    1.28527   53.08079   17.74287   88.37423   18.00751   88.25082   18.14359   88.54266
   17.87895   88.66606   18.09364   89.12646   19.33664   88.54684
```

APPENDIX 3

Notes on Setting Up the Computational Mesh

The mesh spacing in each coordinate direction is specified on input by giving a length and the indices of the first and last mesh points that would occupy that length. If the domain is rotated through the angle of attack, the first length should be the maximum cross-sectional area. The second length is always the initial length of the domain in the y coordinate direction (not the length along the axis). If possible, no part of a domain should contain less than four mesh lines, though less than four may not be harmful if it occurs in only a small portion of the material domain. An aspect ratio of one to one is desirable, though in no case should the aspect ratio be greater than four to one for accurate results. It should be remembered that the mesh for each domain is completely independent of the mesh for any other domain. Once the mesh sizes have been determined, this mesh is defined in the entire region set aside for a material and the material boundary is imbedded in the mesh region. Plots of the meshes generated for each of the materials in case 1 are given as examples of mesh generation.

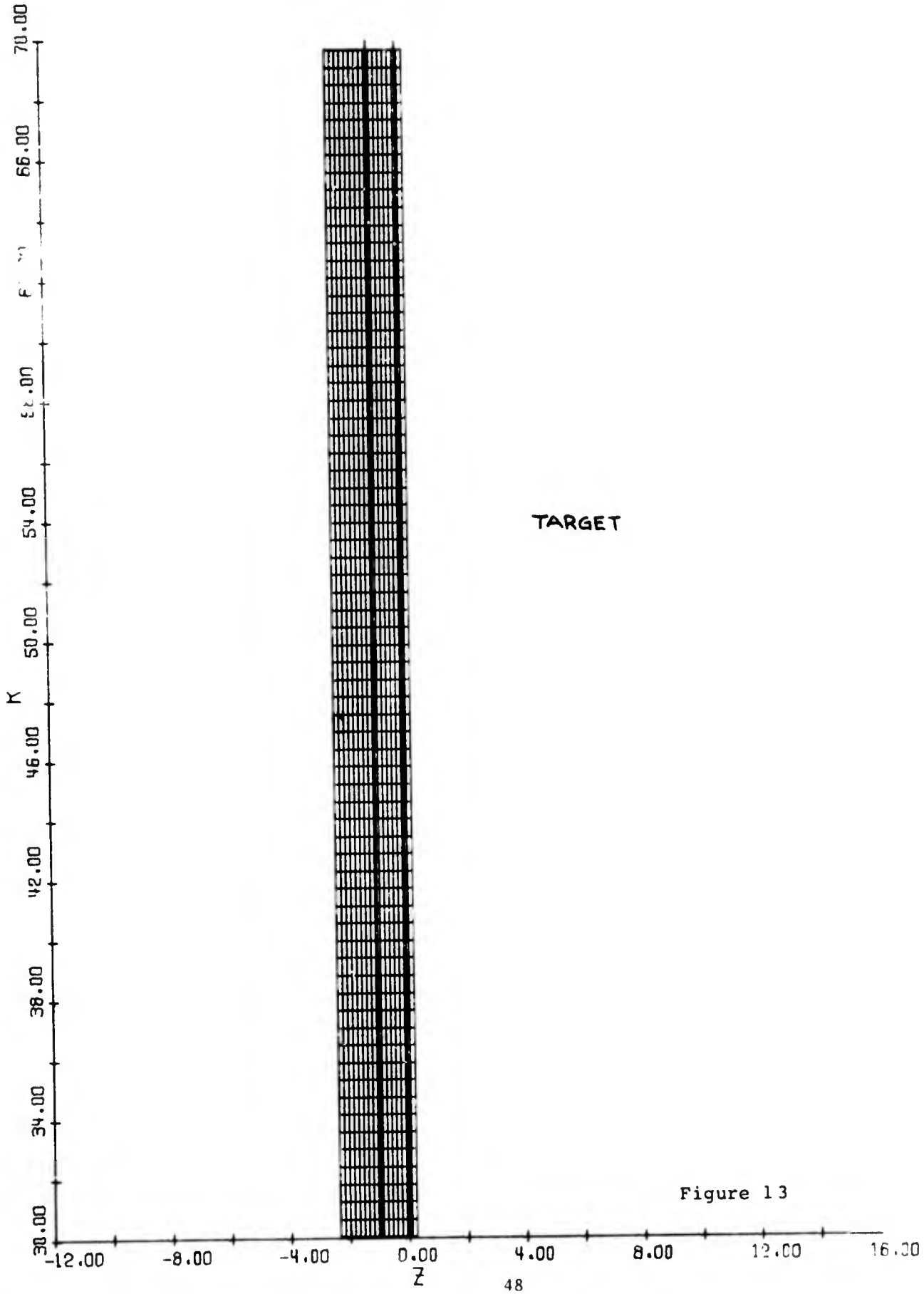
TARGET
70.00
66.00
62.00
58.00
54.00
50.00
46.00
42.00
38.00
34.00
30.00
K
-12.00
-8.00
-4.00
0.00
4.00
8.00
12.00
16.00
Z

Figure 13

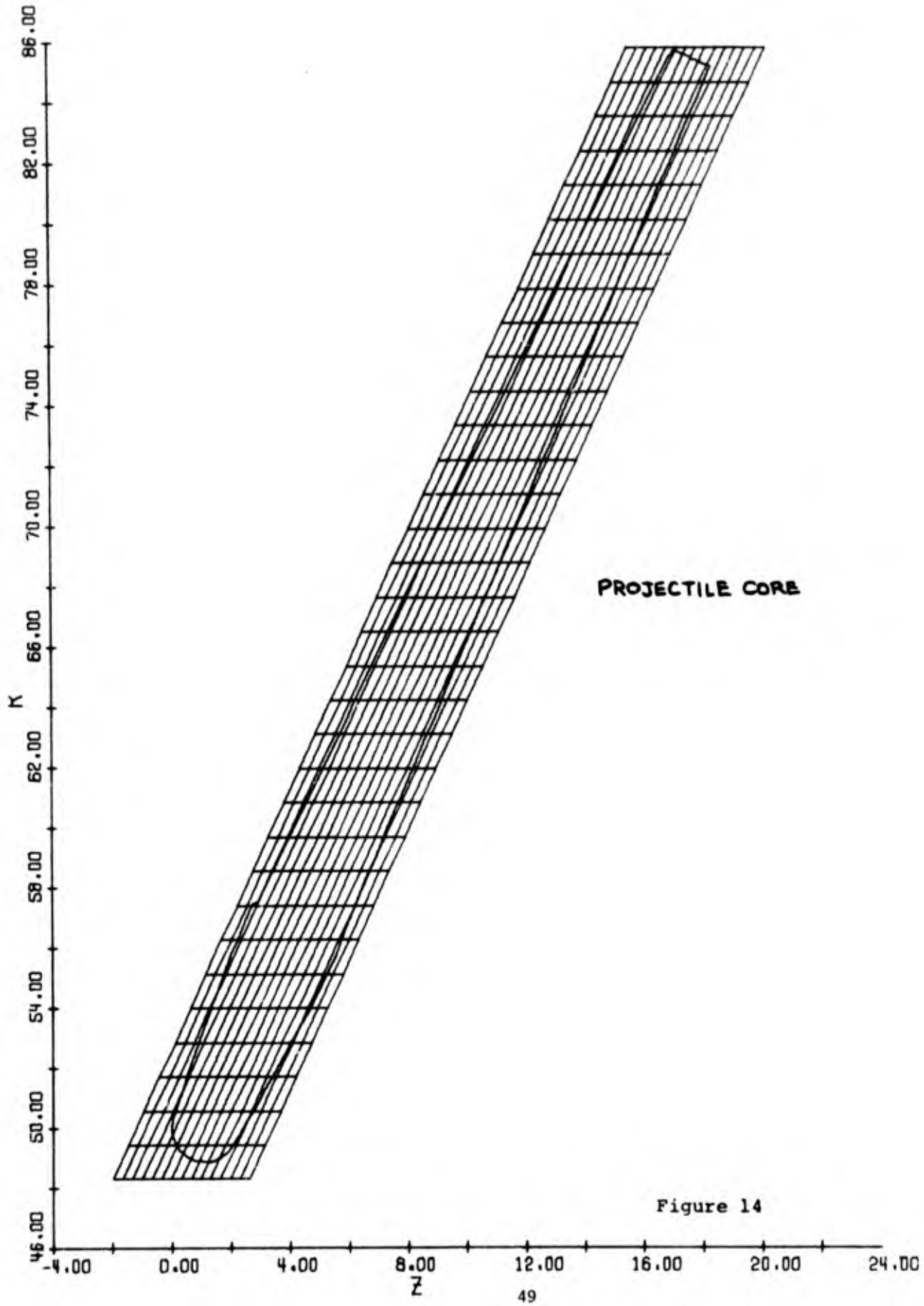
86.00
82.00
78.00
74.00
70.00
66.00
62.00
58.00
54.00
50.00
46.00
X
-4.00
0.00
4.00
8.00
12.00
16.00
20.00
24.00
Z
PROJECTILE CORE

Figure 14

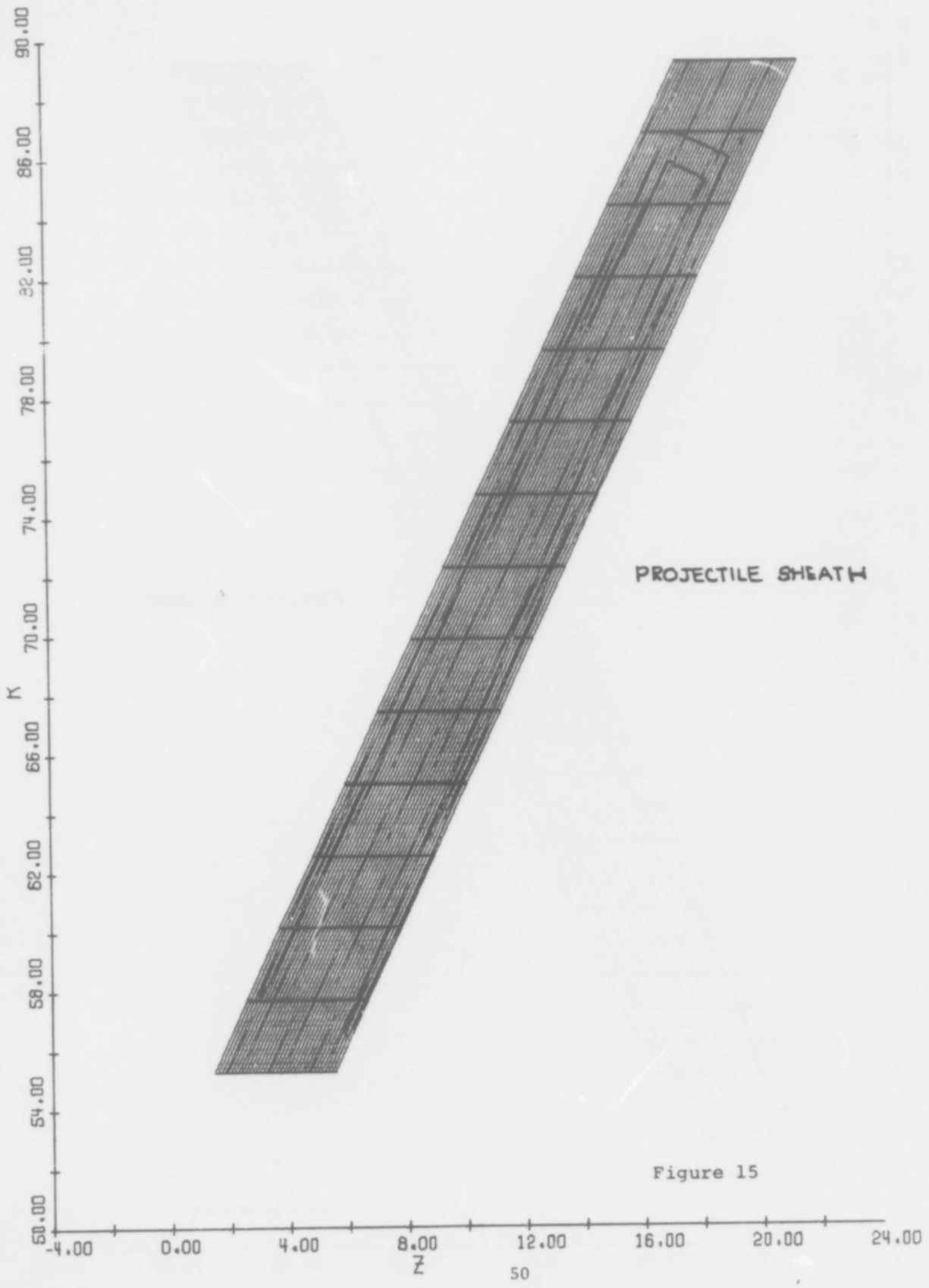
PROJECTILE SHEATH
90.00
86.00
82.00
78.00
74.00
70.00
66.00
62.00
58.00
54.00
50.00
R
-4.00
0.00
4.00
8.00
12.00
16.00
20.00
24.00
Z

Figure 15

APPENDIX 4

Summary of Computations

	Case 1	Case 2
	Silver Bullet	
Projectile mass/ (per unit width)		
core	1600. gm/cm	1100. gm/cm
sheath	188.0 gm/cm	398. gm/cm
Impact Velocity at 65 degrees		
Y-component	-1240. meters/sec	-1388. meters/sec
X-component	- 578.1 meters/sec	- 647. meters/sec
Residual Velocity		
Y-component	-1236.	-1385.2
X-component	- 576.	- 639.6
Target damage		
Estimated hole size	5-6 cm diameter at 20 μ-sec	5-6 cm diameter at 20μ-sec
Hole Shape	Upper surface is a shallow sliced crater with an included angle of approximately 30° measured clockwise from the target face. The upper surface follows the ogive of the core fairly well. Lower surface is a gauge type cut of approximately 125° measured from the target face.	Upper surface moves away from core and therefore makes a steeper angle compared to case 1. Lower surface is similar to case 1.
Estimated Exit Angle of Penetrator	At an increasing angle of attack (>65°)	At a decreasing angle of attack (< 65°)